J|A|C|S
ARTICLES
Published on Web 03/12/2003

Solvent-Sensitive Dyes to Report Protein Conformational Changes in Living Cells

Alexei Toutchkine, Vadim Kraynov, and Klaus Hahn*

Contribution from the Department of Cell Biology, Scripps Research Institute, 10550 North Torrey Pines Road, La Jolla, California 92037

Received October 25, 2002; E-mail: khahn@scripps.edu

Abstract: Covalent attachment of solvent-sensitive fluorescent dyes to proteins is a powerful tool for studying protein conformational changes, ligand binding, or posttranslational modifications. We report here new merocyanine dyes that make possible the quantitation of such protein activities in individual living cells. The quantum yield of the new dyes is sharply dependent on solvent polarity or viscosity, enabling them to report changes in their protein environment. This is combined with other stringent requirements needed in a live cell imaging dye, including appropriate photophysical properties (excitation >590 nm, high fluorescence quantum yield, high extinction coefficient), good photostability, minimal aggregation in water, and excellent water solubility. The dyes were derivatized with iodoacetamide and succinimidyl ester side chains for site-selective covalent attachment to proteins. A novel biosensor of Cdc42 activation made with one of the new dyes showed a 3-fold increase in fluorescence intensity in response to GTP-binding by Cdc42. The dyes reported here should be useful in the preparation of live cell biosensors for a diverse range of protein activities.

Introduction

Cell behavior is regulated through transient activation of protein activities at specific subcellular locations. Our ability to study translocation of proteins has been greatly increased by advances in the microscopy of fluorescent protein analogues within living cells. However, in many cases, localized protein activities are controlled not by translocating proteins to the site of action, but by localized activation of a small portion of the protein pool.[1,2] Such behaviors are not apparent when studying protein translocations or when using in vitro biochemical approaches. Furthermore, the outcome of signaling protein activation can depend on subtle variations in activation kinetics that are not discernible in the population averages generated by biochemical techniques. For precise quantitation of rapid activation kinetics, it is also necessary to measure protein activity in living cells.[2−4] There is a need for tools that can do more than monitor protein movements; biosensors that can quantify the changing subcellular location and level of conformational changes, posttranslational modifications, and/or small ligand binding in vivo will be of great value in cell biology.

Quantifying protein activity in living cells has been accomplished using FRET (fluorescence resonance energy transfer).[1,5,6] The interactions between two proteins have been observed by tagging each with different fluorophores which undergo FRET when the proteins associate.[1,7,8] Alternately, FRET biosensors have been built that bind to a protein only when it adopts a specific conformation. These approaches are very valuable, but FRET-based techniques suffer from limitations that prevent the study of many important targets. Proteins undergoing conformational changes often cannot be "sampled" by a biosensor because the protein is bound to a competing ligand or is incorporated in a multiprotein complex, where it is blocked from biosensor access. Such steric blocking of biosensor access was convincingly demonstrated for the signaling protein Rac, whose activation was not reported in specific subcellular locations because the biosensor had to compete with other proteins.[9] Multiprotein complexes are important targets for live cell biosensors. It is precisely such large, unstable complexes that are difficult to reproduce in vitro and whose transient formation in specific locations must be studied in intact cells. Even when a protein is not sterically blocked, derivatization with a fluorophore near regions of conformational change for FRET can affect biological activity. Finally, because FRET is generated through indirect excitation, it produces a relatively weak fluorescence intensity. This leads to low sensitivity and sometimes the need for complicated methods to differentiate the real signal from autofluorescence or fluorescence of the FRET donor.

(1) Hahn, K.; Toutchkine, A. *Curr. Opin. Cell Biol.* **2002**, *14*, 167−172.
(2) Wouters, F. S.; Verveer, P. J.; Bastiaens, P. I. *Trends Cell Biol*. **2001**, *11*, 203−211.
(3) Williams, D. A.; Fogarty, K. E.; Tsien, R. Y.; Fay, F. S. *Nature* **1985**, *318*, 558−561.
(4) Berridge, M. J. *J Biol. Chem*. **1990**, *265*, 9583−9586.
(5) Pollok, B. A.; Heim, R. *Trends Cell Biol.* **1999**, *9*, 57−60.
(6) Kraynov, V. S.; Chamberlain, C.; Bokoch, G. M.; Schwartz, M. A.; Slabaugh, S.; Hahn, K. M. *Science* **2000**, *290*, 333−337.
(7) Chamberlain, C.; Hahn, K. M. *Traffic* **2000**, *1*, 755−762.
(8) Verveer, P. J.; Wouters, F. S.; Reynolds, A. R.; Bastiaens, P. I. *Science* **2000**, *290*, 1567−1570.
(9) Katsumi, A.; Milanini, J.; Kiosses, W. B.; del Pozo, M. A.; Kaunas, R.; Chien, S.; Hahn, K. M.; Schwartz, M. A. *J. Cell Biol.* **2002**, *158*, 153−164.

10.1021/ja0290882 CCC: $25.00

In this paper we describe new dyes, designed for living cells, which can be used to circumvent these problems. Reporting protein activity using a solvatochromic dye has important advantages complementary to those of FRET. Solvatochromic dyes have been covalently attached to proteins to report a diverse array of protein activities in vitro, including phosphorylation, conformational change, and small ligand binding.[10−19] The use of this approach to study protein activity in vivo is attractive because the solvent-sensitive dye can be attached directly to the protein of interest, producing a fluorescence readout even when the protein is "buried" in a multiprotein complex. Alternately, when using a biosensor that binds to a given conformation of the targeted protein (i.e., an antibody or domain),[1,7,8] no fluorophore is needed on the targeted protein. The biosensor could be labeled with a dye that reflects binding to the targeted protein. This ability to study endogenous, untagged proteins in vivo can be valuable for targets that are not amenable to derivatization. Such proteins include those that cannot be isolated, labeled, and reintroduced in cells or those where important regulatory interactions occur near termini, where GFP would usually be appended. Finally, dyes are directly excited, potentially providing a much brighter signal than FRET.

Dyes typically used in vitro for protein activity studies, including Dansyl, Aedans, Adman etc., have several disadvantages making them difficult to apply in vivo. They fluoresce at short wavelengths, usually much below 400 nm. Irradiation of cells with near-UV light leads to fast cell damage and produces high background from cellular autofluorescence. Fluorophores typically used in living cell (i.e., Fluorescein, Rhodamine, Cyanines, Alexa dyes) must be bright to image very small amounts of material, and the fluorescence intensity of most solvent-sensitive dyes is quite weak compared to such dyes.

In designing the new dyes we focused on merocyanine fluorophores because their spectral properties can be very sensitive to both specific and nonspecific solvent interactions,[20−24] and they can produce very bright fluorescence. In a previous paper one of us described merocyanine dyes which reported calmodulin-calcium binding[25,26] When covalently attached to calmodulin, one such dye reported protein conformational changes in vivo (dye **1a**, Chart 1). However, only relatively hydrophobic dyes could respond well, presumably because attraction to protein hydrophobic regions was necessary for conformational changes to substantially alter the dye's environment. The hydrophobic dyes that were used successfully in the calmodulin analogue were poorly water soluble, greatly reducing their general usefulness. Analogues of other proteins were attempted, but only calmodulin could withstand the high concentrations of organic solvents required for protein labeling with this dye. An equally serious issue was the dye's tendency to form aggregates, typical of merocyanines,[27] which led to serious difficulties during protein labeling and separation of noncovalently attached dye.

Here we describe practical, generally applicable merocyanine dyes that overcome these difficulties. They maintain sufficient hydrophobic character to interact with proteins, yet are water soluble and do not aggregate at concentrations appropriate for protein labeling. The new dyes fluoresce brightly at long wavelengths and show a strong response to solvent/protein environment. They have been derivatized with cysteine- and lysine-selective groups for covalent attachment to proteins. The utility of the new dyes is demonstrated in a novel biosensor for activation of the GTPase protein Cdc42. This biosensor illustrates the potential of solvent-sensitive fluorophores to bind and report activation of endogenous untagged protein.

Results

Merocyanine Dyes with Improved Water Solubility and Reduced Aggregation in Water. We set out initially to make a practical, water-soluble derivative of the dye used in the calmodulin biosensor (Chart 1, original dye = **1a**, new analogues = **1b**−**1h**). A quaternary amino group in that dye was substituted with a much more hydrophilic sulfonato group (−SO_3Na). In some analogues, cysteine-selective iodoacetamido groups were also added for covalent attachment to proteins. The solubility of the sulfonato analogues **1c** and **1d** was significantly improved over the original structure **1a**, and the ability of dye **1d** to attach covalently to cysteine was confirmed by reacting it with β-mercaptoethanol. However, the new dyes still could not be dissolved in aqueous buffers at concentrations suitable for protein labeling. Labeling was accomplished only by including greater than 5% DMSO as cosolvent. Attempts to label a fragment of Wiskott Aldrich Syndrome Protein (WASP) containing a single cysteine showed that it was still very difficult to remove noncovalently bound dye from the labeled protein (dialysis, size exclusion, and ion-exchange chromatography were all unsuccessful).

The protein conjugates contained more than 1 equiv of dye even when labeling was done at low dye concentrations, yet the fluorescence of the conjugates was extremely weak. These data led us to hypothesize that the dyes were forming nonfluorescent H-aggregates in water, as reported previously for other merocyanines.[28−30] These may have been the actual reactive species in aqueous solution. Analysis of dye **1c** absorbance spectra supported the formation of H-aggregates. The spectrum in water differed in shape from spectra in more hydrophobic solvents such as methanol or butanol, and aqueous spectra showed a concentration-dependent shift to a shorter wavelength

(10) Giuliano, K. A.; Taylor, D. L. *Trends Biotechnol.* **1998**, *16*, 135−140.
(11) Cerione, R. A. *Methods Enzymol.* **1994**, *237*, 409−423.
(12) Nomanbhoy, T.; Cerione, R. A. *Biochemistry* **1999**, *38*, 15878−15884.
(13) Nomanbhoy, T.; Cerione, R. A. *Methods Mol. Biol.* **1998**, *84*, 237−247.
(14) Nomanbhoy, T. K.; Cerione, R. *J. Biol. Chem.* **1996**, *271*, 10004−10009.
(15) Baburaj, K.; Azam, N.; Udgaonkar, D.; Durani, S. *Biochim. Biophys. Acta* **1994**, *1199*, 253−265.
(16) Prendergast, F. G.; Meyer, M.; Carlson, G. L.; Iida, S.; Potter, J. D. *J. Biol. Chem.* **1983**, *258*, 7541−7544.
(17) Rasmussen, S. G.; Carroll, F. I.; Maresch, M. J.; Jensen, A. D.; Tate, C. G.; Gether, U. *J. Biol. Chem.* **2001**, *276*, 4717−4723.
(18) Morii, T.; Sugimoto, K.; Makino, K.; Otsuka, M.; Imoto, K.; Mori, Y. *J. Am. Chem. Soc.* **2002**, *124*, 1138−1139.
(19) Daugherty, D.; Gellman, S. *J. Am. Chem. Soc.* **1999**, *121*, 4325−4333.
(20) Brooker, L.; Craig, A.; Heseltine, D.; Jenkins, P.; Lincoln, L. *J. Am. Chem. Soc.* **1964**, *87*, 2443−2450.
(21) Brooker, L.; Keyes, G.; Sprague, R.; VanDyke, R.; VanLare, E.; VanZandt, G.; White, F.; Cressman, H.; Dent, S. *J. Am. Chem. Soc.* **1951**, *73*, 5332−5350.
(22) Buncel, E.; Rajagopal, S. *Acc. Chem. Res.* **1990**, *23*, 226−231.
(23) Reichardt, C. *Solvents and Solvent Effects in Organic Chemistry*, 2nd ed.; VCH Verlagsgesellschaft: Weinheim, 1988.
(24) Liptay, W. *Angew. Chem., Int. Ed. Engl.* **1969**, *8*, 177−188.
(25) Hahn, K. M.; Waggoner, A. S.; Taylor, D. L. *J. Biol. Chem.* **1990**, *265*, 20335−20345.
(26) Hahn, K.; DeBiasio, R.; Taylor, D. L. *Nature* **1992**, *359*, 736−738.
(27) Wurthner, F.; Yao, S.; Debaerdemaeker, T.; Wortmann, R. *J. Am. Chem. Soc.* **2002**, *124*, 9431−9447.
(28) Wurthner, F.; Yao, S. *Angew. Chem., Int. Ed.* **2000**, *39*, 1978−1981.
(29) Lu, L.; Lachicotte, R.; Penner, T.; Perlstein, J.; Whitten, D. *J. Am. Chem. Soc.* **1999**, *121*, 8146−8156.
(30) Valdes-Aguilera, O.; Neckers, D. C. *Acc. Chem. Res.* **1989**, *22*, 171−177.

Chart 1. Structures of Dyes[a]

S-TBA

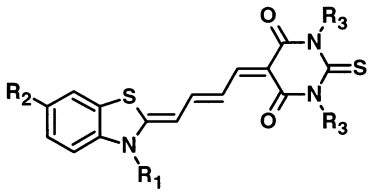

1a: $R_1 = -(CH_2)_3N^+(Me)_2(CH_2)_2NCS$, $R_2 = H$, $R_3 = Bu$

1b: $R_1 = Et$, $R_2 = H$, $R_3 = Me$

1c: $R_1 = -(CH_2)_3SO_3^-$, $R_2 = H$, $R_3 = Me$

1d: $R_1 = -(CH_2)_3SO_3^-$, $R_2 = FmocNH-$, $R_3 = Me$

1e: $R_1 = -(CH_2)_3SO_3^-$, $R_2 = NH_2$, $R_3 = Me$

1f (S-TBA-IAA): $R_1 = -(CH_2)_3SO_3^-$, $R_2 = ICH_2CONH-$, $R_3 = Me$

1g: $R_1 = -(CH_2)_3SO_3^-$, $R_2 = CH_3CONH-$, $R_3 = Me$

1h: $R_1 = -(CH_2)_3SO_3^-$, $R_2 = HO(CH_2)_2SCH_2CONH-$, $R_3 = Me$

S-SO

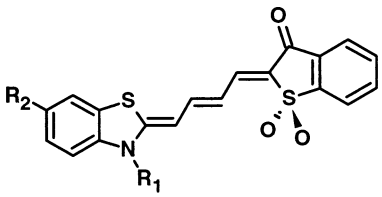

2a: $R_1 = Et$, $R_2 = H$

2b: $R_1 = -(CH_2)_3SO_3^-$, $R_2 = H$

2c: $R_1 = -(CH_2)_3SO_3^-$, $R_2 = FmocNH-$

2d: $R_1 = -(CH_2)_3SO_3^-$, $R_2 = NH_2$

2e (S-SO-IAA): $R_1 = -(CH_2)_3SO_3^-$, $R_2 = ICH_2CONH-$

2f (S-SO-OSu): $R_1 = -(CH_2)_3SO_3^-$, $R_2 = SuOCOCH_2OCH_2CON(CH_3)-$

2g: $R_1 = -(CH_2)_3SO_3^-$, $R_2 = HO(CH_2)_2SCH_2CONH-$

I-TBA

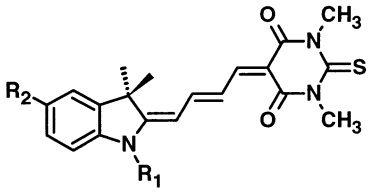

3a: $R_1 = Me$, $R_2 = H$

3b: $R_1 = -(CH_2)_3SO_3^-$, $R_2 = H$

I-SO

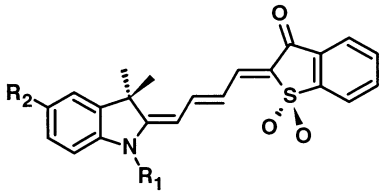

4a: $R_1 = Me$, $R_2 = H$

4b: $R_1 = -(CH_2)_3SO_3^-$, $R_2 = H$

4c: $R_1 = -(CH_2)_3SO_3^-$, $R_2 = FmocNH-$

4d: $R_1 = -(CH_2)_3SO_3^-$, $R_2 = NH_2$

4e (I-SO-IAA): $R_1 = -(CH_2)_3SO_3^-$, $R_2 = ICH_2CONH-$

4f (I-SO-OSu): $R_1 = -(CH_2)_3SO_3^-$, $R_2 = SuOCOCH_2OCH_2CON(CH_3)-$

4g: $R_1 = -(CH_2)_3SO_3^-$, $R_2 = HO(CH_2)_2SCH_2CONH-$

[a] The dyes were named on the basis of the heterocycles on their termini (I = indolenine, S = benzothiazole, TBA = thiobarbituric acid, SO = benzothiophen-3-one-1,1-dioxide).

peak at 515 nm, consistent with the formation of nonfluorescent H aggregates[31] (Figure 1). Furthermore, the excitation and absorbance spectra were different, indicating the presence of multiple species in water (Figure 1). Together, these data suggested that the essentially planar dye was aggregating to reduce the exposure of its hydrophobic surfaces to water, as previously described for other merocyanine dyes.[32]

Such aggregation can be energetically favorable only if the planar dye molecules can get closer to each other than the size of a water molecule. To decrease aggregation, we incorporated bulky, nonplanar substituents with tetragonal geometry in the aromatic rings to make stacking unfavorable (Chart 1). This strategy allowed us to maintain the dyes' relatively hydrophobic

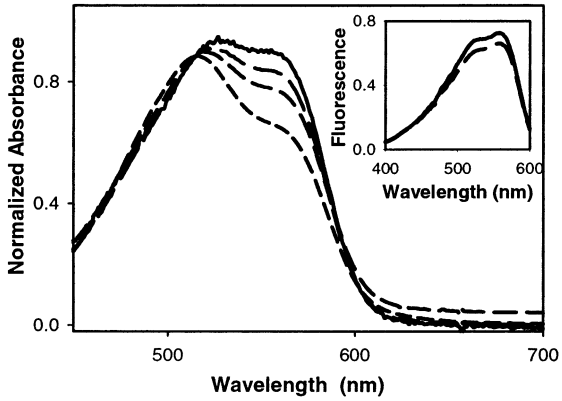

Figure 1. Absorbance and fluorescence (excitation) spectra of S-TBA dye **1c** at different concentrations in water. Concentrations: 1.25 μM (—), 2.5 μM (— —), 12.5 μM (— — —), 25 μM (- - -). Inset: Excitation spectra of dye **1c** in water at 1.25 μM (—) and 2.5 μM (— —).

(31) Mandal, D.; Kumar, S.; Sukul, D.; Bhattacharyya, K. *J. Phys. Chem. A* **1999**, *103*, 8156−8159.
(32) Nakahara, H.; Fukuda, K.; Mobius, D.; Kuhn, H. *J. Phys. Chem.* **1986**, *90*, 6144−6148.

Table 1. Photophysical Properties of Merocyanine Dyes in Various Solvents

dye	solvent	dielectric constant	η,[a] cP	absorption λ_{max}, nm (ϵ[b])	emission λ_{max}, nm	Φ[c]	($\epsilon \times F$)
1b	C_6H_6	2.27	0.604	600 (184 000)	617	0.37	68 000
S-TBA	OcOH	3.4	7.288	598 (220 000)	615	0.52	115 000
	BuOH	17.8	2.544	595 (188 000)	613	0.26	49 000
	MeOH	32.6	0.793	583 (134000)	606	0.13	18 000
	DMF	36.7	0.794	595 (194 000)	613	0.32	62 000
2a	C_6H_6	2.27	0.604	591 (152 000)	617	0.16	24 000
S-SO	OcOH	3.4	7.288	606 (168 000)	623	0.17	29 000
	BuOH	17.8	2.544	604 (163 000)	622	0.12	20 000
	MeOH	32.6	0.793	598 (143 000)	617	0.05	7000
	DMF	36.7	0.794	602 (173 000)	619	0.22	38 000
4a	C_6H_6	2.27	0.604	571 (109 000)	603	0.42	46 000
I-SO	OcOH	3.4	7.288	587 (125 000)	617	0.98	123 000
	BuOH	17.8	2.544	587 (134 000)	618	0.54	72 000
	MeOH	32.6	0.793	586 (143 000)	615	0.08	12 000
	DMF	36.7	0.794	586 (143 000)	615	0.97	140 000
3a	C_6H_6	2.27	0.604	584 (127 000)	605	0.20	26 000
I-TBA	OcOH	3.4	7.288	590 (180 000)	609	0.99	178 000
	BuOH	17.8	2.544	589 (190 000)	609	0.61	116 000
	MeOH	32.6	0.793	583 (173 000)	603	0.26	45 000
	DMF	36.7	0.793	589 (183 000)	611	0.94	172 000

[a] Solvent shear viscosity (from ref 58). [b] Molar extinction coefficient, error ± 5%. [c] Quantum yield of fluorescence, error ± 10%.

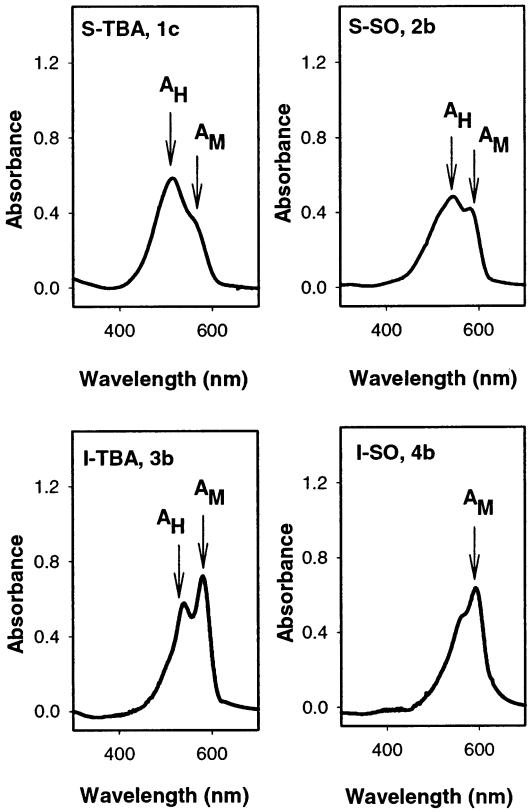

Figure 2. Absorbance of dyes **1c**, **2b**, **3b**, and **4b** in water. All concentrations are equal to 1.0 μM. A_H = absorbance due to aggregation; A_M = absorbance of monomer.

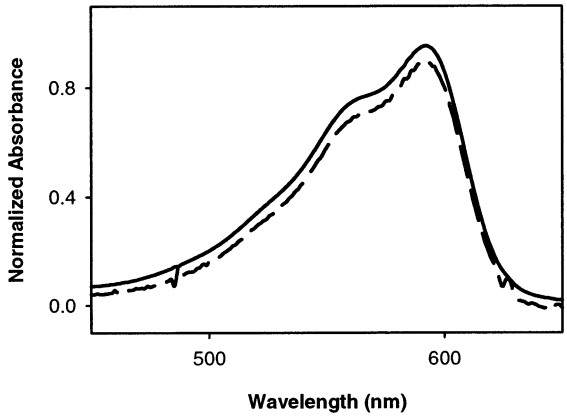

Figure 3. Absorbance of I-SO dye **4b** in water at 1.25 μM (—) and 250 μM (– – –).

character using geminal dimethyl and/or sulfonato groups. The effects of the groups on aggregation were assessed by incorporating them individually or in combination into a series of dyes (**1c**, **2b**, **3b**, **4b**; see Figure 2). Dyes **2b** and **3b** each had one of the tetragonal substituents, while dye **4b** combined both in one structure. As shown in Figure 2, the ratio A_H/A_M (A_H is absorbance of H-aggregates and A_M is absorbance at longer wavelength from monomeric dye) showed that the tetragonal groups strongly decreased aggregation. The aqueous absorbance spectrum of dye **4b**, which contained both out-of-plane substituents, did not depend on concentration, indicating that it did not aggregate even at concentrations greater than 250 μM, well within the range typically used for protein labeling (Figure 3). Introduction of the nonplanar substituents not only reduced aggregation but also greatly improved the dyes' water solubility. Dye **4b** showed excellent water solubility presumably because the substituents made the dye less symmetric and/or because H-aggregation contributes to poor water solubility.

In summary, the new fluorophores showed excellent water solubility and little aggregation and retained substantial hydrophobic character for interaction with proteins. They were named on the basis of the heterocycles at their termini, using a previous nomenclature system (Chart 1).[25]

Attributes for Sensing Protein Activity in Vivo: Spectral Properties and Chemical and Photochemical Stability. The fluorophores in the S-TBA, S-SO, I-TBA, and I-SO dyes all absorb light at long wavelengths advantageous in live cell imaging (Table 1). Their extinction coefficients and quantum yields were characterized in different solvents (Table 1, Figures 4, 5), showing a dramatic solvent-dependent change in fluorescence intensity, which was primarily due to changes in quantum yield. For I-SO, the quantum yield changed more than 12-fold, from 0.97 in DMF to 0.08 in methanol. In the same

Table 2. Absolute Rate Constants of Dye Photobleaching[a]

dye	$k_{ph} \times 10^6$, s^{-1} MeOH	$k_{ph} \times 10^6$, s^{-1} BuOH	Φ_T[b]
I-SO, **4a**	0.28	0.65	
I-TBA, **3a**	0.18	0.78	0.003
S-SO, **2a**	3.0	5.2	
S-TBA, **1b**	4.3	5.2	0.008
Cy5	1.0	0.77	

[a] The error in k_{ph} is ±10%. [b] Quantum yield of triplet state formation in ethanol (from ref 41).

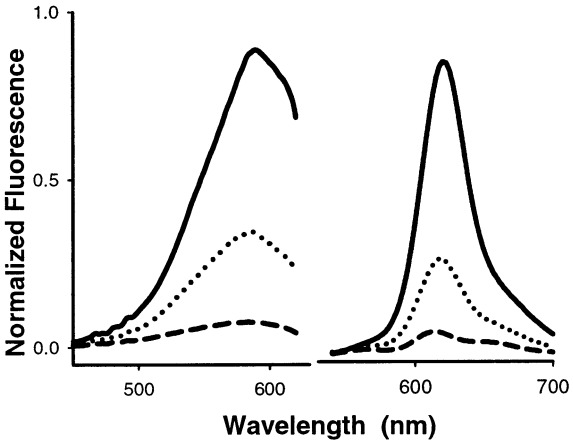

Figure 4. Normalized excitation and emission spectra of S-SO dye **2b** in different solvents: butanol (—), methanol (···), and water (- - -). Excitation spectra acquired with emission at 640 nm. Emission spectra acquired with excitation at 530 nm. C(**2b**) = 0.01 μM.

solvents, S-SO showed a 4.4-fold change in quantum yield. Changes were even greater in water, but this was difficult to quantify precisely for S-SO due to some remaining aggregate formation. The dyes are extraordinarily bright when in a nonpolar environment, comparing very favorably with the brightest dyes currently used in living cells (see Discussion). Although their quantum yields are solvent sensitive, the dyes showed only moderate changes in absorbance and emission maxima with changes of solvent polarity.

Dyes used in living cells must be photostable to provide many sequential images and to obtain sufficient light from minimal amounts of exogenous labeled material. The photostability of the new dyes was characterized by exposing them to constant illumination from a tungsten lamp filtered through glass, a broad spectrum light source that provided essentially equal intensity throughout the spectral range where the dyes would be irradiated in vivo. A fan was used to prevent heating, and dye solutions were adjusted for equal maximal absorbance, kept below 1 μM to minimize the inner filter effect. Photobleaching of dyes **1b**, **2a**, **3a**, and **4a** was compared in two solvents that do not lead to dye aggregation, methanol and butanol, so that all reactions could be attributed to uniformly monomeric dye. Photobleaching followed first-order kinetics in all cases. The bleaching rates were compared to Cy5, a frequently used live cell imaging dye with known photobleaching rates[33] (Table 2, Figure 6). I-SO showed excellent photostability, bleaching with only 28% the rate of Cy5 in methanol.

Bleaching most likely occurred through one of three possible mechanisms, generating reactive oxygen species that destroyed

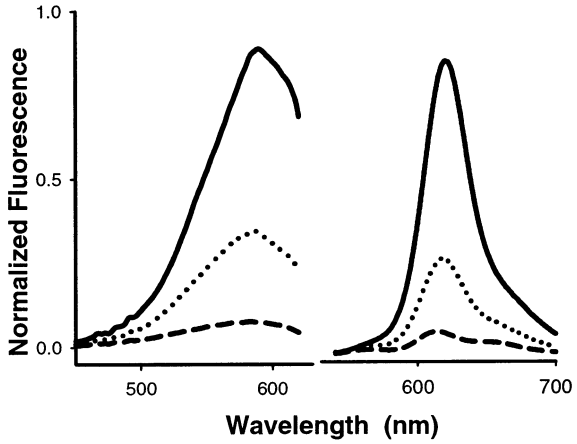

Figure 5. Normalized excitation and emission spectra of I-SO dye **4b** in different solvents: butanol (—), methanol (···), and water (- - -). Excitation spectra acquired with emission at 640 nm. Emission spectra acquired with excitation at 530 nm. C(**4b**) = 0.01 μM.

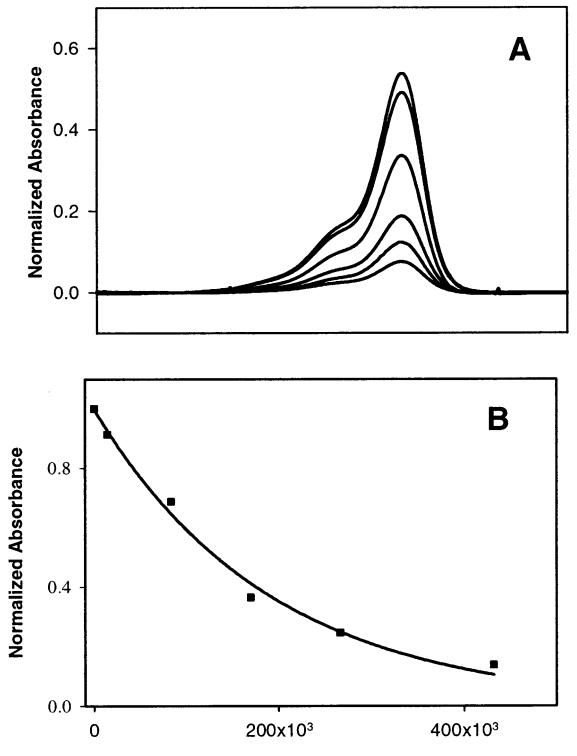

Figure 6. (A) Absorbance spectra of S-TBA dye **1b** (C_0 = 1μM) in butanol after different irradiation times: 0, 3, 23, 47, 74, 120 h. (B) Concentration decay of S-TBA dye **1b** in butanol.

the fluorophore. The triplet excited state of the dye could react with oxygen to produce singlet oxygen, or electron transfer from the singlet excited state dye could generate a reactive oxygen radical anion.[34] The third possible mechanism is a free radical chain reaction between the ground state of the dye and oxygen, initiated by photogenerated peroxides. Although such an autoxidation is common for olefins,[35,36] it is unlikely in our systems, as we did not observe a long induction period or a strong dependence on oxygen concentration.

(33) Toomre, D.; Manstein, D. J. *Trends Cell Biol.* **2001**, *11*, 298−303.
(34) Kanony, C.; Akerman, B.; Tuite, E. *J. Am. Chem. Soc.* **2001**, *123*, 7985−7995.
(35) Collman, J. P.; Kubota, M.; Hosking, J. W. *J. Am. Chem. Soc.* **1967**, *89*, 4809−4811.
(36) Zombeck, A.; Hamilton, D. E.; Drago, R. S. *J. Am. Chem. Soc.* **1982**, *104*, 6782−6784.

To differentiate between the other two possibilities, the reaction was repeated in the presence of thioanisole, a trapping agent that reacts with singlet oxygen or superoxide to produce a sulfoxide or a sulfone.[37,38] Butanol solutions of **1b** generated 90% phenylmethylsulfoxide and 10% phenylmethyl sulfone, consistent with a mechanism mediated by singlet oxygen.[39] Formation of singlet oxygen was also supported by a 7.5-fold increase in bleaching rates upon switching from methanol to deuterated methanol-d_4[40] and by the fact that rates were highest for dyes containing the most sulfur. Sulfur can enhance triplet formation through the inner heavy atom effect.[41,42] Sparging the solution with nitrogen did not affect the rate because very small concentrations of dissolved oxygen are sufficient to saturate the reaction.

Altering the pH between 6 and 9 had no effect on the dye's absorbance, fluorescence intensity, or excitation and emission maxima. Incubation in aqueous buffers at pH 6 or 9 for 3 h at room temperature had no effect.

Derivatives for Site-Specific Protein Labeling. The fluorophores S-SO and I-SO, which showed the most favorable characteristics for live biosensors, were derivatized to make reactive forms which could be site-specifically attached to proteins. Analogues were made with succinimidyl ester for attachment to lysine or with iodoacetamide for selective reaction with cysteine. Use of these groups for site-specific protein labeling is well established.[43]

During synthesis of the reactive dyes (Scheme 1), starting materials carried an amino group, which was used for attachment of side chains at the end of the synthesis. It proved challenging to find an amine protecting group which could survive the quaternization reaction in the initial steps of the synthesis, yet could be removed without destroying the completed fluorophore. This hurdle was overcome using novel deprotection conditions for the Fmoc group, which could be cleanly removed with sodium acetate in dimethyl sulfoxide (rather than the stronger bases such as piperidine which are usually used). A 3-sulfonatopropyl substituent was also incorporated in each dye during these syntheses to further enhance water solubility.

Attachment of reactive side chains affected the quantum yields of both S-SO and I-SO dyes (Table 3). Although all side chains were attached to the fluorophore via an amide linkage, the effects were very different for each side chain and fluorophore. For example, when adding succinimidyl esters to the fluorophores, the quantum yield in methanol did not change for S-SO, yet decreased 38% for I-SO. The iodoacetamido group decreased the quantum yield of both fluorophores (32% decrease for S-SO, 87% decrease for I-SO in methanol). Such a large decrease in the brightness of the I-SO iodoacetamido would severely limit its utility. We hoped the decrease was caused by the presence of iodine, which is known to quench fluorescence.[44] Iodine is lost during the reaction with protein, so this source of reduction in quantum yield would not be a problem. We therefore tested the effect of iodine by reacting the I-SO and S-SO dyes with β-mercaptoethanol (dyes **2g**, **4g**, Table 3), which returned the quantum yield of S-SO to that of the underivatized fluorophore, and that of I-SO to half that of the unaltered fluorophore.

To further explore the mechanisms by which amine substituents affected quantum yield, S-TBA dyes bearing different substitutents were characterized (Table 4). Attachment of an underivatized amino group directly to the fluorophore reduced the dye's extinction coefficient by 63% and the quantum yield by >13-fold. However, this effect was nearly eliminated when the amine was acetylated, as in the final reactive dye derivatives (see Discussion).

Scheme 1. Synthesis of dyes **1b**−**1e**; **2a**−**2f**; **3a**,**b**; **4a**−**4f**.

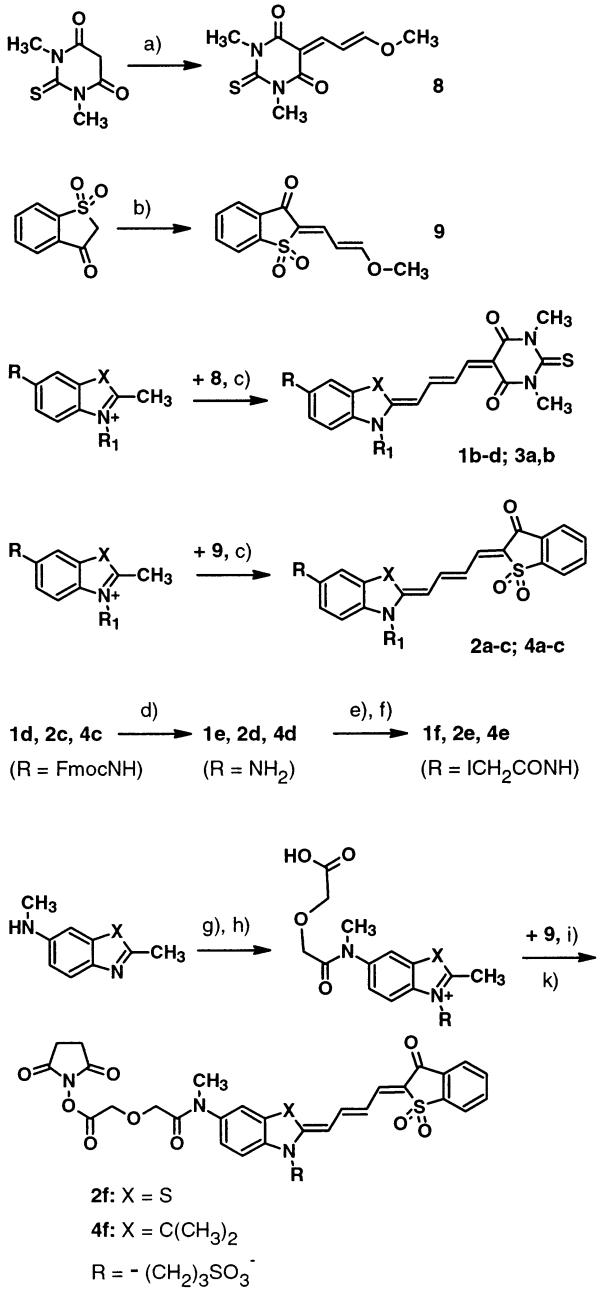

[a] Conditions: (a) 1,3,3-trimethoxypropene, MeOH, reflux. (b) 1,3,3-trimethoxypropene, 90 °C. (c) AcONa, MeOH-$CHCl_3$, reflux. (d) AcONa, DMSO, 100 °C. (e) $ClCH_2COCl/Et_3N$, DMF, −40 °C. (f) NaJ, MeOH, reflux. (g) Diglycolic anhydride, $CHCl_3$, reflux. (h) propanesultone, C_6H_6, 75 °C. (i) AcONa, AcOH, 80 °C. (k) TSTU/(*i*-Pf)$_2$EtN, DMF, rt.

(37) Foote, C. S.; Peters, J. W. *J. Am. Chem. Soc.* **1971**, *93*, 3795−3796.
(38) Correa, P. E.; Hardy, G.; Riley, D. P. *J. Org. Chem.* **1988**, *53*, 1695−1702.
(39) Watanabe, Y.; Kuriki, N.; Ishiguro, K.; Sawaki, Y. *J. Am. Chem. Soc.* **1991**, *113*, 2677−2682.
(40) Wasserman, H., Ed. *Singlet Oxygen*; Academic Press: New York, 1979; Vol. 40.
(41) Benniston, A.; Gulliya, K.; Harriman, A. *J. Chem. Soc., Faraday Trans.* **1997**, *93*, 2491−2501.
(42) Turro, N. J. *Tetrahedron* **1985**, *41*, 2089−2098.
(43) Dent, A.; Aslam, M. *Bioconjugation* **1998**, 364−482.

Table 3. Photophysical Properties of Reactive Forms of Merocyanine Dyes

dye	solvent	absorption, λ_{max} nm (ϵ^a)	emission, λ_{max} nm	Φ^b	($\epsilon\times\phi$)
2e	H_2O	552, 592	618	*c*	*c*
S-SO-IAA	MeOH	610 (140 000)	628	0.034	3000
	BuOH	618 (160 000)	636	0.06	9600
2f	H_2O	552, 591	618	*c*	*c*
S-SO-OSu	MeOH	603 (142 000)	621	0.06	9000
	BuOH	608 (134 000)	626	0.12	28000
2g	MeOH	610 (138 000)	629	0.054	8000
S-SO-βME					
4e	H_2O	599 (143 000)	630	0.004	600
I-SO-IAA	MeOH	601 (138 000)	634	0.01	1400
	BuOH	607 (150 000)	639	0.06	9000
4f	H_2O	594 (150 000)	616	0.01	1500
I-SO-OSu	MeOH	586 (140 000)	620	0.05	7000
	BuOH	590 (134 000)	623	0.19	26000
4g	H_2O	600 (140 000)	620	0.02	3000
I-SO-βME	MeOH	601 (140 000)	621	0.04	6000
	BuOH	609 (142 000)	628	0.12	17000

[a] Molar extinction coefficient, error ±5%. [b] Quantum yield of fluorescence, error ±10%. [c] Not determined because of aggregation in water.

Table 4. Spectral Properties of Substituted S-TBA Dyes in Methanol

dye	absorption, λ_{max}/nm (ϵ^a)	emission, λ_{max}/nm	Φ^b
1b S-TBA-H	586 (112 000)	601	0.13
1e S-TBA-NH_2	594 (42 000)	628	0.01
1g S-TBA-$NHCOCH_3$	595 (108 000)	616	0.11

[a] Molar extinction coefficient, error is ±5%. [b] Quantum yield of fluorescence, error is ±10%.

S-SO in a Biosensor of Cdc42 Activation. The ability of the S-SO dye to respond to changes in protein environment was demonstrated by using it to make a novel biosensor of Cdc42 activation. Wiskott Aldrich Syndrome Protein (WASP) binds only to the activated, GTP-bound form of Cdc42, not to the GDP-bound form.[45] A fragment of WASP that retains this selective binding ability (residues **201**−**320** in the original protein) was derivatized with S-SO dye **2e**. Guided by the crystal structure of the WASP−Cdc42 complex,[46] a cysteine was introduced into the fragment to attach the dye where it could interact with several hydrophobic amino acids (F271C mutation of WASP fragment). The labeled WASP fragment showed a 300% increase in fluorescence intensity when incubated with activated Cdc42, but not with GDP-bound, inactive Cdc42 (Figure 7). Moreover, the apparent equilibrium binding constant for Cdc42 (150 ± 50 nM) was measured in vitro by titrating a fixed concentration of the labeled WASP fragment with various amounts of cdc42-GTPγS. This value is in good agreement with the published data[47] (133 ± 9 mM) for the WASP−Cdc42 interaction and indicative that the binding properties of the WASP domain were not greatly affected by incorporation of the solvent-sensitive fluorophore into the WASP fragment. This biosensor and its biological applications will be described in detail elsewhere.

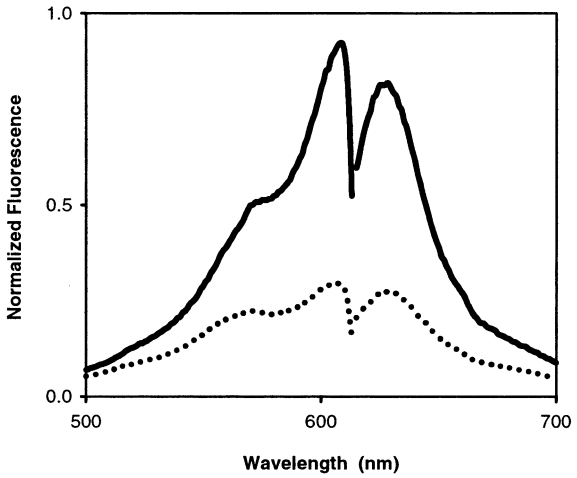

Figure 7. Excitation and emission spectra of the S-SO-WASP fragment in the presence of GDP−Cdc42 (···) and GTPγS−Cdc42 (—). Excitation spectra were acquired with emission at 630 nm, emission spectra with excitation at 600 nm. [CBD] = 150 nM, [Cdc42] = 300 nM, [GNP] = 10 μM.

Discussion

This paper describes new fluorescent dyes that can be used to study previously inaccessible protein activities in living cells. Solvent-sensitive dyes suitable for imaging in vivo can be attached directly to proteins, where they will report conformational changes even when the proteins are sterically blocked from access by domains or antibodies such as those used in many current biosensors.[1,7] As demonstrated by the new Cdc42 biosensor we describe here, such dyes can also be used on domain- or antibody-based biosensors to report activation of endogenous, untagged proteins. Direct excitation of the dye can provide substantially brighter signals than is generated by FRET.

Spectral Properties Valuable for Live Cell Biosensors. Solvent-sensitive dyes commonly used in vitro are poorly suited for use in living cells. They are not sufficiently bright to quantify spectral changes from small amounts of labeled protein, and their short excitation and emission wavelengths damage cells and overlap cellular autofluorescence. To be bright and fluoresce at longer wavelengths, dyes must have extended conjugation, which unfortunately reduces water solubility and leads to self-aggregation. The frequently used dyes designed for use in living cells were specifically selected to be insensitive to their environment, because they are used to quantify protein distribution (i.e., Fluorescein, Rhodamine, Alexa, Cy3/5). In such dyes, solubility problems could be overcome by incorporating charged groups around the dyes' edges. This was not desirable in our dyes, which must retain interactions with hydrophobic protein regions to report protein conformational changes. Dyes must interact with the protein surface so that protein conformational changes affect their interactions with water, hydrogen bonding, or hydrophobic interactions. For domain- or antibody-based sensors, dyes must be able to move from water to hydrophobic pockets during protein binding events. The limited previous examples where solvatochromic dyes were used to monitor protein activity in vivo were restricted to proteins that could be labeled with hydrophobic dyes in organic cosolvents.[25]

For the new dyes described here, solubility problems were overcome while maintaining hydrophobic moieties for protein

(44) McGlynn, S. P.; Azumi, T.; Kinoshita, M. *Molecular Spectroscopy of the Triplet State*; Prentice Hall: Englewood Cliffs, NJ, 1969.
(45) Machesky, L.; Insall, R. *J. Cell. Biol.* **1999**, *146*, 267−272.
(46) Abdul-Manan, N.; Aghazadeh, B.; Liu, G.; Majumdar, A.; Ouerfelli, O.; Siminovitcch, K.; Rosen, M. *Nature* **1999**, *399*, 379−383.
(47) Kim, A. S.; Kakalis, L. T.; Abdul-Manan, N.; Liu, G. A.; Rosen, M. K. *Nature* **2000**, *404*, 151−158.

interaction. We incorporated aliphatic or weakly charged substituents which projected out of the plane of the aromatic ring to generate merocyanines that were water soluble and showed minimal or no aggregations at concentrations used for protein labeling. Screening structures containing such out-of-plane groups led to the identification of two fluorophores, S-SO and I-SO, which had both the desired solubility and excellent solvent-sensitive spectral properties for reporting protein conformational changes in vivo.

I-SO showed a more than 12-fold change in fluorescence intensity ($\epsilon^*\Phi$, Table 1) in DMF vs methanol, and S-SO showed a 5.4-fold change in the same solvents. Changes of this magnitude are much larger than any seen in live cell biosensors to date. However, solvents do not accurately reflect the protein environments the dyes will experience. The magnitude of changes produced in different solvents is useful for comparing different structures and demonstrates potential maximum changes and dye brightness in a biosensor. Nonetheless, it was important to show that the S-SO dye underwent a 3-fold change in florescence intensity in an actual biosensor, the indicator of Cdc42 activation described here. This change is substantially better than that of the majority of biosensors used successfully in living cells to date.

The Achilles heel of the new dyes is that they report protein activity through a change in fluorescence intensity. This presents difficulties during imaging, in that the intensity of the dye will depend not only on the biosensor response but also on cell thickness, uneven illumination, and other artifacts. Such problems have been overcome in other applications using well-established imaging techniques, in which the cell is loaded with a fluorophore that is not sensitive to environment.[48−50] The changing intensity of the biosensor is normalized against this second fluorophore, which corrects for cell volume, illumination, etc. Perhaps more importantly, on a protein the dye will not experience the large changes in environment encountered in different solvents, and its actual response is difficult to predict. We have found that I-SO and S-SO, when attached to proteins, show a conformational-dependent shift between two intensities falling somewhere within the range seen during our solvent dependence studies. These two intensities were sometimes bright and in other cases fell in the low end of the dyes' potential intensity range.

The brightness of the dye will vary depending on the protein used and the local environment at the attachment position. When in nonpolar solvents, both I-SO and S-SO are extraordinarily bright. If brightness is taken as the product of the molar extinction coefficient and the quantum yield, the new fluorophores can be seen to compare very favorably with other dyes, not sensitive to environment, that are in common use today: I-SO, 140000 (DMF); S-SO, 38000 (DMF); Rhodamine B, 52000 (ethanol); Cy3, 7000 (ethanol). The published values used here for commercially available dyes were obtained in polar solvents because these dyes were designed to be very water soluble and to be immersed in water rather than interacting with protein. Published values for solvent-sensitive fluorophores are substantially dimmer than those of the new dyes reported here, i.e., Aedans, 4000 (methanol), 7000 (DMF)[51]; Adman, 9000 (methanol), 3000 (chloroform).[52]

Scheme 2. Mechanisms of dye photodegradation.

Mechanism 1:

$$\text{Dye} + h\nu \longrightarrow {}^1\text{Dye}^{\bullet} \quad (1)$$

$${}^1\text{Dye}^* + \text{O}_2 \longrightarrow \text{Dye}^{\bullet+} + \text{O}_2^{\bullet-} \quad (2)$$

$$\text{Dye} + \text{O}_2^{\bullet-} \longrightarrow \text{Products} \quad (3)$$

Mechanism 2:

$$\text{Dye} + h\nu \longrightarrow {}^1\text{Dye}^* \xrightarrow[\text{crossing}]{\text{intersystem}} {}^3\text{Dye}^* \quad (1)$$

$${}^3\text{Dye}^* + {}^3\text{O}_2 \longrightarrow \text{Dye} + {}^1\text{O}_2 \quad (2)$$

$$\text{Dye} + {}^1\text{O}_2 \longrightarrow \text{Products} \quad (3)$$

Chemical and Photochemical Stability; Bleaching Mechanism. The dyes showed excellent chemical stability and insensitivity to pH changes over the physiological range. Photobleaching rates were compared with those of Cy5, a dye with proven capacity for long-term imaging in vivo, for which photostability data have been published. Both I-SO and S-SO showed sufficient photostability for extended studies in cells, and I-SO bleached more slowly than Cy5.

Our data support an oxygen-assisted photobleaching mechanism, in which the triplet excited state of the dye reacts with triplet oxygen to produce singlet oxygen, a highly reactive species that destroys the fluorophore (see Scheme 2). We carried out several studies to differentiate between this mechanism and the alternate oxygen-assisted mechanism, in which the singlet excited state of the dye reacts with oxygen to form a dye radical cation and an oxygen radical anion (superoxide), another highly reactive species. The importance of these two mechanisms for photobleaching depends on the relative rates of the electron transfer step (step 2, mechanism 1 in Scheme 2) versus formation of the triplet state (step 1, mechanism 2). Photobleaching rates were not strongly dependent on oxygen concentrations. Because triplet oxygen can react with the triplet excited state of the dye even at extremely low concentrations, this is consistent with singlet oxygen formation. Trapping experiments with thioanisole demonstrated the formation of singlet oxygen. The slower bleaching in methanol than in butanol supported singlet-oxygen formation, as electron transfer would have been increased in more polar solvents. Photobleaching rates were greater for dyes with more sulfur (S-SO and S-TBA), also consistent with bleaching mediated by singlet oxygen. Heavy atoms such as sulfur increase the probability of singlet−triplet intersystem crossing and promote singlet-oxygen

(48) Bright, G. R.; Fisher, G. W.; Rogowska, J.; Taylor, D. L. *J. Cell Biol.* **1987**, *104*, 1019−1033.
(49) Bright, G. R.; Fisher, G. W.; Rogowska, J.; Taylor, D. L. *Methods Cell Biol.* **1989**, *30*, 157−192.
(50) DeBiasio, R. L.; LaRocca, G. M.; Post, P. L.; Taylor, D. L. *Mol. Biol. Cell* **1996**, *7*, 1259−1282.
(51) Hudson, E. N.; Weber, G. *Biochemistry* **1973**, *12*, 4154−4161.
(52) Jacobson, A.; Petric, A.; Hogenkamp, D.; Sinur, A.; Barrio, J. *J. Am. Chem. Soc.* **1996**, *118*, 5572−5579.

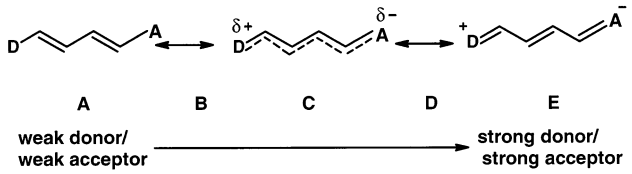

Figure 8. Resonance structures of merocyanine dyes.

formation. The relative rates of S-TBA vs I-TBA bleaching are consistent with their quantum yields for triplet state formation (Table 2). The dyes absorbing at longer wavelengths (S-SO and S-TBA) bleached faster. This was inconsistent with the radical anion mechanism involving formation of an oxygen radical anion, which would be facilitated by higher energy excited states. Finally, the photooxidation of S-TBA in deuterated methanol-d_4 was 7.5-fold faster than in methanol; the lifetime of singlet oxygen is longer in deuterated solvents.[40] Understanding the bleaching mechanism will be important in designing improved dyes in the future.

Basis of Solvent-Dependent Spectral Changes. An ideal dye would report protein conformation through changes in its excitation or emission maxima, rather than its intensity. This would eliminate the need for a second, "volume indicator" fluorophore for normalization of the signal. Understanding the basis of spectral changes for the current dyes will be important in designing such an improved dye in the future.

The ground state of merocyanine dyes can be represented as a resonance hybrid between charged and noncharged forms (Figure 8). In any given solvent, the contribution of each resonance form depends on the relative donor and acceptor strength of the two aromatic rings at the termini of the dye. As described by Marder and others,[53−56] if both the donor and acceptor are weak, the molecular structure will be effectively like an unperturbed polyene (structure **A** in Figure 8). With increasing donor and/or acceptor strength the ground state structure becomes both more dipolar and more delocalized, becoming a fully delocalized, cyanine-like structure (**C** in Figure 8). Further increase in the donor or acceptor strength leads toward the limit of a fully charge-separated structure (**E**) where the double bonds are again localized, but their position is shifted from structure **A**. By varying the terminal groups, intermediate structures throughout the range can be produced (i.e., **B** and **D**).

In the so-called cyanine limit **C**, the ground and excited states are each characterized by equal contributions from the two resonance forms.[56,57] Dyes at the cyanine limit are characterized by equal dipole moments in the ground and excited states, such that solvents affect both states similary and there is minimal solvent-dependent change in the fluorescence maxima. Furthermore, these excitation and emission maxima reach the longest wavelengths at the cyanine limit.[23]

Because our dyes show only moderate solvatochromism, it is reasonable to assume that they are near the cyanine limit. In hydrogen-bonding solvents, the excitation maxima of all the dyes shifted to shorter wavelengths as solvent polarity increased (normal alcohols of decreasing chain length). By contrast, in non-hydrogen bonding solvents the maxima shifted in the opposite direction for all but the S-TBA dye. This is presumably because the hydrogen-bonding solvents stabilized the polar resonance forms of the dyes, placing the resonance hybrid somewhere in region **D**. Increasing solvent polarity shifted the structure further toward **E** and away from state **C**, which has the longest wavelength excitation maximum. Most of the dyes in the non-hydrogen-bonding solvents were closer to state **B**. Increasing the solvent polarity in that case brought them closer to the cyanine limit **C**, thereby increasing the wavelength of the excitation maxima. Only the S-TBA dye, which is a combination of the strongest donor and the strongest acceptor, showed a different behavior in aprotic solvents. It was likely in region **D** even in aprotic solvents and so was shifted away from the cyanine limit as solvent polarity increased.

The large solvent-dependent changes in the fluorescence intensity of the dyes were due largely to changes in quantum yield, rather than to changes in the efficiency of absorbance. Photoisomerization about the central double bonds, frequently the predominant deexcitation pathway for merocyanines, is affected by viscosity and solvent polarity. With the exception of one solvent tested, the quantum yield increased as solvent hydrophobicity and viscosity increased, consistent with known effects on double-bond isomerization.[31] In contrast, quantum yields in DMF were higher than those in butanol, even though butanol has a lower dipole moment and is more viscous than DMF. Hydrogen bonding in the excited state has been shown to bring about efficient radiationless deactivation for Merocyanine 540 and Nile Red, possibly due to stabilization of zwitterionic forms, which enhance photoisomerization,[58] or due to the availability of additional paths for vibrational deexcitation.[59] The difference between butanol and DMF can be attributed to effects of hydrogen bonding. It would be very advantageous for the dyes to respond to hydrogen bonding, as this can enable them to report relatively small protein conformational changes which affect hydrogen bonds. Remarkably, the I-SO and S-SO fluorophores were much more sensitive to viscosity than solvent polarity. This is consistent with structures near the cyanine limit, as cyanine dyes respond to viscosity but much less to solvent polarity.

Derivatization of the fluorophores for attachment of reactive side chains strongly affected fluorescence. When the dyes were derivatized with amine "handles" for attachment of side chains, the amino group substantially reduced quantum yields (13-fold reduction for S-TBA dye **1e** vs **1b**). Brightness was restored when the amine was derivatized with succinimidyl ester side chains. The quenching was likely due to photoinduced electron transfer between the amine and the fluorophore, as has been observed for similar structures.[60] When the amine was substituted with electron-withdrawing substituents (i.e., amido substituted dye **1e**), electron transfer was reduced and fluorescence increased. A reduction in quantum yield was also observed when an iodoacetamido group, used for cysteine labeling, was

(53) Bublitz, G.; Ortiz, R.; Marder, S.; Boxer, S. *J. Am. Chem. Soc.* **1997**, *119*, 3365−3376.
(54) Ortiz, R.; Marder, S.; Cheng, L.-T.; Tiemann, B.; Cavagnero, S.; Ziller, J. *J. Chem. Soc., Chem. Commun.* **1994**, 2263−2264.
(55) Blanchard-Desce, M.; Wortmann, R.; Lebus, S.; Lehn, J.-M.; Kramer, P. *Chem. Phys. Lett.* **1995**, *243*, 526−532.
(56) Würthner, F.; Wortmann, R.; Meerholz, K. *CHEMPHYSCHEM* **2002**, *3*, 17−31.
(57) Würthner, F.; Wortmann, R.; Matschiner, R.; Lukaszuk, K.; Meerholz, K.; DeNardin, Y.; Bittner, R.; Brauchle, C.; Sens, R. *Angew. Chem, Int. Ed. Engl.* **1997**, *36*, 2765−2768.
(58) Onganer, Y.; Yin, M.; Bessire, D.; Quitevis, E. *J. Phys. Chem.* **1993**, *97*, 2344−2354.
(59) Czer, A.; Nagy, K.; Biczok, L. *Chem. Phys. Lett.* **2002**, *360*, 473−478.
(60) de Silva, A. P.; Gunaratne, H. Q. N.; Gunnlaugsson, T.; Huxley, A. J. M.; McCoy, C. P.; Rademacher, J. T.; Rice, T. E. *Chem. Rev.* **1997**, *97*, 1515−1566.

included. We hypothesized that this was due to iodine, a heavy atom that is known to enhance formation of the triplet excited state, thus reducing fluorescence. As the iodine is eliminated during reaction with protein, this presented no real practical difficulties. Reaction of the iodoacetamido dyes with mercaptoethanol increased the quantum yield as expected, though in the case of I-SO not back to the levels of the unsubstituted dye. The reasons for the quenching of the I-SO carrying the thioether side chain remain unclear.

Biosensor Application of the S-SO dye. The utility of the dyes was proven by using them to build a new biosensor that reported activation of endogenous, untagged Cdc42. By examining the crystal structure of the WASP−Cdc42 complex, we were able to identify hydrophobic pockets formed when the two proteins bound. S-SO was attached to an amino acid that would place it in this pocket when a WASP fragment bound to Cdc42. This fragment bound only to activated, GTP-bound Cdc42, producing a 3.0-fold change in fluorescence intensity. Such a change can be readily detected in vivo.

In control experiments where the WASP fragment was labeled with Cy3 and Cy5 fluorophores, no change in fluorescence intensity was observed. These dyes are known to experience a large increase in fluorescence intensity when transferred to more hydrophobic or more viscous environments, but are not sensitive to hydrogen bonding with the solvent.[61,62] Thus, the lack of response with the cyanine-labeled WASP fragments suggests that our dyes are responding to a change in hydrogen bonding, as they move into the hydrophobic pocket and decrease exposure to water.

This biosensor demonstrates the feasibility of using the dyes to study the many proteins that cannot be modified without severely affecting their biological activity. Thus, the approach provides a valuable alternative in living cells. The dyes will also be valuable when attached directly to proteins, enabling conformational changes to be followed in vivo for proteins incorporated in large molecular machines. For in vitro applications, the dyes provide a substantially brighter signal than current solvent-sensitive fluorophores. Thus they can enhance sensitivity for studying high-affinity binding interactions, small amounts of protein in high-throughput assays, or protein changes that produce only small effects on other dyes. We hope that these studies will lay a foundation for the development of even better dyes that can reflect protein conformation through changes in their excitation and emission maxima, while remaining brightly fluorescent.

Experimental Section

General Aspects. Analytical grade reagents were purchased from major suppliers. UV−vis spectra were measured using a Hewlett-Packard 8453 diode array spectrophotometer. Emission and excitation spectra were obtained using a Spex Fluorolog 2 spectrofluorometer at 23 °C. Quantum yields were measured using merocyanine 540[58] as an internal standard.[63] Solutions were not deaerated because control experiments showed that oxygen did not quench the fluorescence of these dyes, due perhaps to their short lifetimes. Mass spectra were obtained on an IonSpec FT MS spectrometer (MALDI-FT MS), Hewlett-Packard 5890 gas chromatograph equipped with a 5971A mass selective detector (MS-EI), and Hewlett-Packard 1100 high-performance liquid chromatograph equipped with a 1100 mass selective detector (MS-ESI). ^{1}H spectra of 0.5% solutions in $CDCl_3$ or CD_3SOCD_3 were recorded on Bruker DRX-400 or DRX-500 spectrometers. The peaks corresponding to the residual protons of $CDCl_3$ (7.27 ppm) or CD_3SOCD_3 (2.49 ppm) were used as internal reference. All operations with dyes were performed under dim light. Flasks containing dyes were wrapped with aluminum foil.

3-(2,3,3-Trimethyl-3*H*-indolium-1-yl)propane-1-sulfonate (**5**),[64] 3-(2-methyl-1,3-benzothiazol-3-ium-3-yl)propane-1-sulfonate (**6**),[65] 3-ethyl-2-methyl-1,3-benzothiazol-3-ium iodide (**7**),[66] 1-benzothiophen-3(2*H*)-one 1,1-dioxide,[67] 2,3,3-trimethyl-3*H*-indol-5-amine,[68] and 2-methyl-1,3-benzothiazol-6-amine[69] were prepared as previously reported. Chemical names for compounds were obtaining using ACD/ChemSketch software.[70]

5-[(2*E*)-3-Methoxyprop-2-enylidene]-1,3-dimethyl-2-thioxodihydropyrimidine-4,6(1*H*,5*H*)-dione (8). 1,3,3-Trimethoxypropene (1.32 g, 10 mmol) was added rapidly to a boiling solution of 1,3-dimethyl-2-thiobarbituric acid (1.29 g, 7.5 mmol) in 10 mL of a $CHCl_3$−MeOH (1:1) mixture. Reflux was continued for 5 min, and the solution was cooled to room temperature. The solid formed was filtered, washed with a small amount of MeOH, and dried. The yield was 1.20 g (75%). ^{1}H NMR (400 MHz, $CDCl_3$): δ 3.71 (s, 6H, 2×CH_3), 3.96 (s, 3H, OCH_3), 7.48 (t, $^3J_{H-H}$ = 12.5 Hz, 1H), 7.56 (d, $^3J_{H-H}$ = 12.5 Hz, 1H), 8.11 (d, $^3J_{H-H}$ = 12.5 Hz, 1H). GC−MS (70 eV) *m*/*e* (relative intensity): 240 (100, M^+), 209 (25, $(M - OCH_3)^+$).

(2*E*)-2-[(2*E*)-3-Methoxyprop-2-enylidene]-1-benzothiophen-3(2*H*)-one 1,1-Dioxide (9). A mixture of 1,3,3-trimethoxypropene (2.64 g, 20 mmol) and 1.82 g (10 mmol) of 1-benzothiophen-3(2*H*)-one 1,1-dioxide was heated at 90 °C for 12 h. The solid formed was recrystallized from MeOH to give 1.88 g (75% yield) of final product. ^{1}H NMR (400 MHz, $CDCl_3$): δ 4.02 (s, 3H, OCH_3), 6.51 (t, $^3J_{H-H}$ = 12.3 Hz, 1H), 7.51−8.11 (m, 6H). GC-MS (70 eV) *m*/*e* (relative intensity): 250 (65, M^+), 219 (100, $(M - OCH_3)^+$)

General Procedure A (Dyes 3a, 4a). 2-Methylene-1,3,3-trimethylindolenine (300 mg, 1.9 mmol) was added at once to a boiling solution of 500 mg (2.00 mmol) of enol ether **8** or **9** in 5.0 mL of a methanol−chloroform mixture (1:1). The reaction mixture was stirred at reflux for 30 min. After cooling, the dye separated as a crystalline solid. The dye was additionally purified by recrystallization from methanol.

1,3-Dimethyl-2-thioxo-5-[(2*E*,4*Z*)-4-(1,3,3-trimethyl-1,3-dihydro-2*H*-indol-2-ylidene)but-2-enylidene]dihydropyrimidine-4,6(1*H*,5*H*)-dione (3a). The yield was 75%. ^{1}H NMR (500 MHz, $CDCl_3$): δ 1.74 (s, 6H, $C(CH_3)_2$), 3.56 (s, 3H, NCH_3), 3.88 (s, 6H, 2×CH_3), 6.09 (d, $^3J_{H-H}$ = 12.5 Hz, 1H), 7.06−8.22 (m, 6H). MALDI-FTMS: MH^+ found 382.1584, expected 382.1584.

(2*Z*)-2-[(2*E*,4*Z*)-4-(1,3,3-Trimethyl-1,3-dihydro-2*H*-indol-2-ylidene)-but-2-enylidene]-1-benzothiophen-3(2*H*)-one 1,1-Dioxide (4a). The yield was 68%. ^{1}H NMR (500 MHz, DMSO-d_6): δ 1.70 (s, 6H, $C(CH_3)_2$), 3.60 (s, 3H, NCH_3), 6.33 (d, $^3J_{H-H}$ = 13.6 Hz, 1H), 6.71 (t, $^3J_{H-H}$ = 13.2 Hz, 1H), 7.2−8.0 (m, 8H), 8.28 (t, $^3J_{H-H}$ = 13.6 Hz, 1H). MALDI-FTMS: MH^+ found 392.1313, expected 392.1315.

General Procedure B (Dyes 1b, 1c, 2a, 2b, 3b, 4b). Indolium or benzothiazolium salt (**5**, **6**, or **7**, 1.00 mmol) was added at once to a boiling solution of enol ether **8** or **9** (500 mg, 2.0 mmol) in 5.0 mL of a methanol−chloroform mixture (1:1) followed by addition of 100 mg of sodium acetate. The reaction mixture was stirred at reflux for 30 min. After cooling, the dye separated as a crystalline solid. The dye was additionally purified by recrystallization from methanol.

(61) Soper, S. A.; Mattingly, Q. L. *J. Am. Chem. Soc.* **1994**, *116*, 3744−3752.
(62) Ischenko, A. *Russ. Chem. Rev.* **1991**, *60*, 865−884.
(63) Demas, J. N.; Crosby, G. A. *J. Phys. Chem.* **1971**, *75*, 991−1024.
(64) Flannagan, J. H.; Khan, S. H.; Menchen, S.; Soper, S. A.; Hammer, R. P. *Bioconj. Chem.* **1997**, *8*, 751−756.
(65) Lednev, I. K.; Fydorova, O. A.; Gromov, S. P.; Alfimov, M. V. *Spectrochim. Acta, Part A* **1993**, *49A*, 1055−1056.
(66) Narayanan, N.; Patonay, G. *J. Org. Chem.* **1995**, *60*, 2391−2395.
(67) Regitz, M. *Chem. Ber.* **1965**, *98*, 36−45.
(68) Mujumdar, R. B.; Ernst, L. A.; Mujumdar, S. R.; Waggoner, A. S. *Cytometry* **1989**, *10*, 11−19.
(69) Manning, W. B.; Horak, V. *Synthesis* **1978**, *5*, 363.
(70) Advanced Chemistry Development Inc.: Toronto, Canada.

1,3-Dimethyl-5-[(2*E*,4*E*)-4-(3-ethyl-1,3-benzothiazol-2(3*H*)-ylidene)-but-2-enylidene]-2-thioxodihydropyrimidine-4,6(1*H*,5*H*)-dione (1b). The yield was 85%. ^{1}H NMR (500 MHz, $CDCl_3$): δ 1.55 (t, $^3J_{H-H}$ = 6.6 Hz, 3H, CH_3), 3.86 (s, 6H, 2×CH_3), 4.26 (q, $^3J_{H-H}$ = 6.6 Hz, 2H, CH_2N), 6.27 (d, $^3J_{H-H}$ = 12.8 Hz, 1H), 7.40−8.06 (m, 7H). MALDI-FTMS: MH^+ found 386.0989, expected 386.0991.

Sodium 3-[(2*E*)-2-[(2*E*)-4-(1,3-Dimethyl-4,6-dioxo-2-thioxotetrahydropyrimidin-5(2*H*)-ylidene)but-2-enylidene]-1,3-benzothiazol-3(2*H*)-yl]propane-1-sulfonate (1c). The yield was 82%. ^{1}H NMR (500 MHZ, $CDCl_3$): δ 2.03 (p, $^3J_{H-H}$ = 7.0 Hz, 2H, $CH_2CH_2CH_2$), 2.60 (t, $^3J_{H-H}$ = 7.0 Hz, 2H, CH_2SO_3), 3.58 (s, 6H, 2×CH_3), 4.61 (t, $^3J_{H-H}$ = 7.0 Hz, 2H, CH_2N), 6.91 (d, $^3J_{H-H}$ = 13.6 Hz, 1H), 7.40−8.06 (m, 7H). MALDI-FTMS MH^+ found 502.0545; expected 502.0536.

(2*Z*)-2-[(2*E*,4*E*)-4-(3-Ethyl-1,3-benzothiazol-2(3*H*)-ylidene)but-2-enylidene]-1-benzothiophen-3(2*H*)-one 1,1-Dioxide (2a). The yield was 70%. ^{1}H NMR (400 MHz, DMSO-d_6): δ 1.29 (t, $^3J_{H-H}$ = 6.6 Hz, 3H, CH_3), 4.40 (q, $^3J_{H-H}$ = 6.6 Hz, 2H, CH_2N), 6.57 (t, $^3J_{H-H}$ = 13.6 Hz, 1H), 6.71 (d, $^3J_{H-H}$ = 13.6 Hz, 1H), 7.3−7.8 (m, 10H). MALDI-FTMS: MH^+ found 396.0728, expected 396.0723.

Sodium 3-[(2*E*)-2-[(2*E*,4*Z*)-4-(1,1-Dioxido-3-oxo-1-benzothien-2(3*H*)-ylidene)but-2-enylidene]-1,3-benzothiazol-3(2*H*)-yl]propane-1-sulfonate (2b). The yield was 67%. ^{1}H NMR (500 MHz, DMSO-d_6): δ 1.85 (p, $^3J_{H-H}$ = 7.0 Hz, 2H, $CH_2CH_2CH_2$), 2.60 (t, $^3J_{H-H}$ = 7.0 Hz, 2H, CH_2SO_3), 4.44 (t, $^3J_{H-H}$ = 7.0 Hz, 2H, CH_2N), 6.67 (t, $^3J_{H-H}$ = 12.8 Hz, 1H), 6.87 (d, $^3J_{H-H}$ = 13.2 Hz, 1H), 7.40−8.10 (m, 10H). ESI-MS: 490 (M − Na + 2H)$^+$.

Sodium 3-{(2*Z*)-2-[(2*E*)-4-(1,3-Dimethyl-4,6-dioxo-2-thioxotetrahydropyrimidin-5(2*H*)-ylidene)but-2-enylidene]-3,3-dimethyl-2,3-dihydro-1*H*-indol-1-yl}propane-1-sulfonate (3b). The yield was 70%. ^{1}H NMR (500 MHz, $CDCl_3$): δ 1.74 (s, 6H, $C(CH_3)_2$), 2.05 (p, $^3J_{H-H}$ = 7.0 Hz, 2H, $CH_2CH_2CH_2$), 2.63 (t, $^3J_{H-H}$ = 7.0 Hz, 2H, CH_2SO_3), 3.67 (s, 6H, 2×CH_3), 4.34 (t, $^3J_{H-H}$ = 7.0 Hz, 2H, CH_2N), 6.58 (d, $^3J_{H-H}$ = 12.6 Hz, 1H), 7.2−8.4 (m, 7H). ESI-MS: 490 (M − Na + 2H)$^+$.

Sodium 3-{(2*Z*)-5−2-[(2*E*,4*Z*)-4-(1,1-Dioxido-3-oxo-1-benzothien-2(3*H*)-ylidene)but-2-enylidene]-3,3-dimethyl-2,3-dihydro-1*H*-indol-1-yl}propane-1-sulfonate (4b). The yield was 65%. ^{1}H NMR (500 MHz, DMSO-d_6): δ 1.74 (s, 6H, $C(CH_3)_2$), 2.05(p, $^3J_{H-H}$ = 7.0 Hz, 2H, $CH_2CH_2CH_2$), 2.63 (t, $^3J_{H-H}$ = 7.0 Hz, 2H, CH_2SO_3), 4.25(t, $^3J_{H-H}$ = 7.0 Hz, 2H, CH_2N), 6.47 (d, $^3J_{H-H}$ = 13.6 Hz, 1H), 6.72 (t, $^3J_{H-H}$ = 13.2 Hz, 1H), 7.2−8.4 (m, 10H). ESI-MS: 500 (M − Na + 2H)$^+$.

Preparation of Thiol-Reactive S-TBA-IAA (1f), S-SO-IAA (2e), and I-SO-IAA (4e) Dyes. 9*H*-Fluoren-9-ylmethyl 2-Methyl-1,3-benzothiazol-6-ylcarbamate (10). A 1.64 g (0.01 mol) sample of 2-methyl-6-aminobenzothiazole was added in small portions to 40 mL of a 1:1 mixture of FMOC−Cl in chloroform (2.59 g, 0.01 mol) and saturated aqueous sodium bicarbonate solution at room temperature. After addition was completed, stirring was continued for 1 h. The organic layer was separated, washed with water (2 × 20 mL), and dried over $MgSO_4$. The solvent was removed in a vacuum, and the solid residue was recrystallized from methanol to give 3.0 g (80%) of protected amine. ^{1}H NMR (400 MHz, $CDCl_3$): δ 2.79 (s, 3H, CH_3), 4.27 (t, $^3J_{H-H}$ = 6.2 Hz, 2H, OCH_2), 4.58 (d, $^3J_{H-H}$ = 6.2 Hz, 1H, CH) 6.8−7.8 (m, 11H, aromatic rings), 8.3 (bs, 1H, NH). ESI-MS: 387 (MH^+).

9*H*-Fluoren-9-ylmethyl 2,3,3-trimethyl-3*H*-indol-5-ylcarbamate (11). The title compound was prepared by the same method as **10**. Protected amine was purified by chromatography on silica using dichloromethane as eluent. The yield was 2.85 g (72%). ^{1}H NMR (400 MHz, $CDCl_3$): δ 2.79 (s, 3H, CH_3), 4.27 (t, $^3J_{H-H}$ = 6.2 Hz, 2H, OCH_2), 4.58 (d, $^3J_{H-H}$ = 6.2 Hz, 1H, CH) 6.8−7.8 (m, 11H, aromatic rings), 8.3 (bs, 1H, NH). ESI-MS: 397 (MH^+).

9*H*-Fluoren-9-ylmethyl 2-Methyl-3-(3-sulfonatopropyl)-1,3-benzothiazol-6-ylcarbamate (12). A mixture of 8 mmol of protected amine and 1,3-propane sulfone (1.83 g, 15 mmol) in 10 mL of 1,2-dichlorobenzene was heated at 120 °C for 12 h. The solid was filtered and washed with hot benzene and hot methanol to produce a white solid. The yield was 3.45 g (87%). ^{1}H NMR (500 MHz, DMSO-d_6): δ 2.18 (p, $^3J_{H-H}$ = 6.2 Hz, 2H, $CH_2-CH_2-CH_2$), 2.68 (t, $^3J_{H-H}$ = 6.2 Hz, 2H, CH_2-SO_3), 3.20 (s, 3H, CH_3), 4.42 (t, $^3J_{H-H}$ = 6.6 Hz, 1H, $CH-CH_2$), 4.66 (d, $^3J_{H-H}$ = 6.6 Hz, 2H, $CH-CH_2$), 4.91 (t, t, $^3J_{H-H}$ = 6.2 Hz, 2H, CH_2-N), 7.3−8.5 (m, 10H), 10.34 (bs, 1H). ESI-MS: 509 (MH^+).

3-(5-{[(9*H*-Fluoren-9-yloxy)carbonyl]amino}-2,3,3-trimethyl-3*H*-indolium-1-yl)propane-1-sulfonate (13). The title compound was prepared by the same method as **12**. The yield was 80%. ^{1}H NMR (500 MHz, DMSO-d_6): δ 1.55 (s, 6H, 2×CH_3), 2.21 (p, $^3J_{H-H}$ = 6.2 Hz, 2H, $CH_2-CH_2-CH_2$), 2.70 (t, $^3J_{H-H}$ = 6.2 Hz, 2H, CH_2-SO_3), 2.84 (s, 3H, CH_3), 4.40 (t, $^3J_{H-H}$ = 6.6 Hz, 1H, $CH-CH_2$), 4.56 (d, $^3J_{H-H}$ = 6.6 Hz, 2H, $CH-CH_2$), 4.67 (t, $^3J_{H-H}$ = 6.2 Hz, 2H, CH_2-N), 7.3−8.1 (m, 10H), 10.34 (bs, 1H). ESI-MS: 519 (MH^+).

Preparation of Protected Dyes 1d, 2c, and 4c. The dyes were prepared using general procedure B from quaternary salt **12** or **13** and enol ether **8** or **9**.

Sodium 3-[(2*Z*)-{[(9*H*-Fluoren-9-yloxy)carbonyl]amino}-2-[(2*E*)-4-(1,3-dimethyl-4,6-dioxo-2-thioxotetrahydropyrimidin-5(2*H*)-ylidene)-but-2-enylidene]-1,3-benzothiazol-3(2*H*)-yl] propane-1-sulfonate (1d). The yield was 90%. ^{1}H NMR (500 MHz, DMSO-d_6): δ 2.09 (p, $^3J_{H-H}$ = 7.0 Hz, 2H, $CH_2-CH_2-CH_2$), 2.49 (t, $^3J_{H-H}$ = 7.0 Hz, 2H, CH_2-SO_3), 3.66 (s, 6H, 2×CH_3), 4.40 (t, $^3J_{H-H}$ = 6.2 Hz, 1H, $CH-CH_2$), 4.60−4.70 (m, 4H, $CH-CH_2$, $N-CH_2$), 6.8−8.5 (m, 15H), 10.15 (bs, 1H). MALDI-FTMS: MH^+ found 739.1343, expected 739.1325.

Sodium 3-[(2*E*)-6-{[(9*H*-Fluoren-9-yloxy)carbonyl]amino}-2-[(2*E*,4*Z*)-4-(1,1-dioxido-3-oxo-1-benzothien-2(3*H*)-ylidene)but-2-enylidene]-1,3-benzothiazol-3(2*H*)-yl]propane-1-sulfonate (2c). The yield was 85%. ^{1}H NMR (500 MHz, DMSO-d_6): δ 2.03 (p, $^3J_{H-H}$ = 7.0 Hz, 2H, $CH_2-CH_2-CH_2$), 2.61 (t, $^3J_{H-H}$ = 7.0 Hz, 2H, CH_2-SO_3), 4.39 (t, $^3J_{H-H}$ = 6.2 Hz, 1H, $CH-CH_2$), 4.50−4.70 (m, 4H, CH_2-N, $CH-CH_2$), 6.5−8.0 (m, 19H), 10.2 (bs, 1H). MALDI-FTMS: MH^+ found 749.1033, expected 749.1056.

Sodium 3-{(2*Z*)-5-{[(9*H*-Fluoren-9-yloxy)carbonyl]amino}-2-[(2*E*,4*Z*)-4-(1,1-dioxido-3-oxo-1-benzothien-2(3*H*)-ylidene)but-2-enylidene]-3,3-dimethyl-2,3-dihydro-1*H*-indol-1-yl}propane-1-sulfonate (4c). The yield was 90%. ^{1}H NMR (500 MHz, DMSO-d_6): δ 1.67(s, 6H, 2×CH_3), 2.05 (p, $^3J_{H-H}$ = 7.0 Hz, 2H, $CH_2-CH_2-CH_2$), 2.65 (t, $^3J_{H-H}$ = 7.0 Hz, 2H, CH_2-SO_3), 4.24 (t, $^3J_{H-H}$ = 7.0 Hz, 2H, CH_2-N), 4.38 (t, $^3J_{H-H}$ = 6.6 Hz, 1H, $CH-CH_2$), 4.54 (d, $^3J_{H-H}$ = 6.6 Hz, 2H, $CH-CH_2$), 6.4−8.5 (m, 19H), 9.95 (bs, 1H). ESI-MS: 737.2 (M − Na + 2H)$^+$.

General Procedure for Deprotection of Fmoc Group. Preparation of Dyes 1e, 2d, and 4d. A mixture of Fmoc-protected dye (1.00 mmol) and sodium acetate (10 mg, 0.12 mmol) in 15 mL of dimethyl sulfoxide was stirred at 100 °C for 10 min. The mixture was cooled to 20 °C, and the dye was precipitated by addition of 50 mL of diethyl ether. The dye was used without further purification in the next step.

Sodium 3-[(2*Z*)-6-Amino-2-[(2*E*)-4-(1,3-dimethyl-4,6-dioxo-2-thioxotetrahydropyrimidin-5(2*H*)-ylidene)but-2-enylidene]-1,3-benzothiazol-3(2*H*)-yl]propane-1-sulfonate (1e). The yield was 93%. ^{1}H NMR (400 MHz, DMSO-d_6): δ 2.00 (p, $^3J_{H-H}$ = 7.0 Hz, 2H, $CH_2-CH_2-CH_2$), 2.55 (t, $^3J_{H-H}$ = 7.0 Hz, 2H, CH_2-SO_3), 3.61 (s, 6H, 2×CH_3), 4.56 (t, $^3J_{H-H}$ = 7.0 Hz, 2H, CH_2-N), 5.83 (s, 2H, NH_2), 6.8−7.8 (m, 7H). ESI-MS: 495 (M − Na + 2H)$^+$.

Sodium 3-[(2*E*)-6-Amino-2-[(2*E*,4*Z*)-4-(1,1-dioxido-3-oxo-1-benzothien-2(3*H*)-ylidene)but-2-enylidene]-1,3-benzothiazol-3(2*H*)-yl]-propane-1-sulfonate (2d). The yield was 95%. ^{1}H NMR (500 MHz, DMSO-d_6): δ 2.08 (p, $^3J_{H-H}$ = 7.0 Hz, 2H, $CH_2-CH_2-CH_2$), 2.64 (t, $^3J_{H-H}$ = 7.0 Hz, 2H, CH_2-SO_3), 4.57 (t, $^3J_{H-H}$ = 7.0 Hz, 2H, CH_2-N), 5.78 (s, 2H, NH_2), 6.4−7.8 (m, 11H). ESI-MS: 505 (M − Na + 2H)$^+$.

Sodium 3-{(2*Z*)-5-Amino-2-[(2*E*,4*Z*)-4-(1,1-dioxido-3-oxo-1-benzothien-2(3*H*)-ylidene)but-2-enylidene]-3,3-dimethyl-2,3-dihydro-1*H*-indol-1-yl}propane-1-sulfonate (4d). The yield was 80%. ^{1}H NMR

(500 MHz, DMSO-d_6): δ 1.58(s, 6H, 2×CH_3), 2.03 (p, $^3J_{H-H}$ = 6.2 Hz, 2H, $CH_2-CH_2-CH_2$), 2.63 (t, $^3J_{H-H}$ = 6.2 Hz, 2H, CH_2-SO_3), 4.24 (t, $^3J_{H-H}$ = 6.2 Hz, 2H, CH_2-N), 5.42 (s, 2H, NH_2), 6.4−8.5 (m, 11H). ESI-MS: 515 $(M - Na + 2H)^+$.

Sodium 3-{(2*Z*)-5-[(Iodoacetyl)amino]-2-[(2*E*,4*Z*)-4-(1,1-dioxido-3-oxo-1-benzothien-2(3*H*)-ylidene)but-2-enylidene]-3,3-dimethyl-2,3-dihydro-1*H*-indol-1-yl}propane-1-sulfonate (I-SO-IAA, 4e). A solution of chloroacetyl chloride (200 mg, 1.78 mmol) in 2 mL of DMF was added dropwise to a cooled (−40 °C) solution of 250 mg (0.47 mmol) of dye **21** and 100 mg of triethylamine in 10 mL of DMF. After addition was completed, the reaction mixture was stirred at −40 °C for an additional hour. Methanol (10 mL) was added to the reaction mixture, and the temperature was slowly raised to room temperature. Diethyl ether was added to the mixture to precipitate the dye. The crude dye was chromatographed over silica gel, eluting with acetone−methanol (3:1) to yield 201 mg (70%) of pure chloroacetamido dye. This dye was refluxed in 10 mL of methanol containing 600 mg of sodium iodide for 3 h. The solution was cooled, filtered, and concentrated in a vacuum to 5 mL. The dye was precipitated by addition of 50 mL of acetone, filtered, and dried. The dye was purified by recrystallization from methanol. The yield was 209 mg (63% based on starting dye **21**). ^{1}H NMR (500 MHz, DMSO-d_6): δ 1.69 (s, 6H, $C(CH_3)_2$), 2.03 (p, $^3J_{H-H}$ = 7.0 Hz, 2H, $CH_2-CH_2-CH_2$), 2.63 (t, $^3J_{H-H}$ = 7.0 Hz, 2H, CH_2-SO_3), 3.91 (s, 2H, CH_2I), 4.24 (t, $^3J_{H-H}$ = 7.0 Hz, 2H, CH_2-N), 6.4−8.3 (m, 11H), 10.53 (s, 1H, NH). MALDI−FTMS: MH^+ found 705.0219, calculated 705.0197.

Sodium 3-[(2*Z*)-2-[(2*E*)-4-(1,3-Dimethyl-4,6-dioxo-2-thioxotetrahydropyrimidin-5(2*H*)-ylidene)but-2-enylidene]-6-[(iodoacetyl)-amino]-1,3-benzothiazol-3(2*H*)-yl]propane-1-sulfonate (S-TBA-IAA, 1f). The dye was prepared using the same method as for dye **4e** starting from dye **1e.** The dye was purified by recrystallization from methanol. The yield was 65%. ^{1}H NMR (400 MHz, DMSO-d_6): δ 2.07 (p, $^3J_{H-H}$ = 7.0 Hz, 2H, $CH_2-CH_2-CH_2$), 2.61 (t, $^3J_{H-H}$ = 7.0 Hz, 2H, CH_2-SO_3), 3.57 (s, 6H, 2×CH_3), 3.93 (s, 2H, CH_2I), 4.59 (t, $^3J_{H-H}$ = 7.0 Hz, 2H, CH_2-N), 6.8−8.5 (m, 7H), 10.5 (s, 1H, NHCO). ESI-MS: 663 $(M - Na + 2H)^+$.

Sodium 3-[(2*E*)-6-[(Iodoacetyl)amino]-2-[(2*E*,4*Z*)-4-(1,1-dioxido-3-oxo-1-benzothien-2(3*H*)-ylidene)but-2-enylidene]-1,3-benzothiazol-3(2*H*)-yl]propane-1-sulfonate (S-SO-IAA, 2e). The dye was prepared using the same method as for dye **4e** starting from dye **2d.** The dye was purified by recrystallization from methanol. The yield was 60%. ^{1}H NMR (500 MHz, DMSO-d_6): δ 2.08 (p, $^3J_{H-H}$ = 7.0 Hz, 2H, $CH_2-CH_2-CH_2$), 2.67 (t, $^3J_{H-H}$ = 7.0 Hz, 2H, CH_2-SO_3), 3.93 (s, 2H, CH_2I), 4.57 (t, $^3J_{H-H}$ = 7.0 Hz, 2H, CH_2-N), 6.6−8.5 (m, 11H), 10.74 (s, 1H, NHCO). MALDI−FTMS: MH^+ found 694.9431, expected 694.9448.

Preparation of Amino-Reactive I-SO-OSu (4f) and S-SO-OSu (2f) Dyes. *N*-(2,3,3-Trimethyl-3*H*-indol-5-yl)acetamide (14) and *N*-(2-Methyl-1,3-benzothiazol-6-yl)acetamide (15). Amine (2,3,3-trimethyl-3*H*-indol-5-amine or 2-methyl-1,3-benzothiazol-6-amine), 3 mmol, was mixed with acetic anhydride (10 mL), and the mixture was heated at 60 °C for 20 min. The solvents were evaporated in a vacuum, and the residue was purified by recrystallization from alcohol (benzothiazole derivative) or by column chromatography on silica using ethyl acetate as eluent (indolenine derivative).

***N*-(2,3,3-Trimethyl-3*H*-indol-5-yl)acetamide.** The yield was 60%, yellow powder. ^{1}H NMR (400 MHz, $CDCl_3$): δ 1.26 (s, 6H, 2×CH_3), 2.15 (s, 3H, $COCH_3$), 2.24 (s, 3H, CH_3), 6.8−7.8 (m, 3H, aromatic ring), 8.0 (bs, 1H, NH). ESI-MS: 217 (MH^+).

***N*-(2-Methyl-1,3-benzothiazol-6-yl)acetamide.** The yield was 80%, white powder. ^{1}H NMR (500 MHz, $CDCl_3$): δ 2.27 (s, 3H, $COCH_3$), 2.86 (s, 3H, CH_3), 7.3−8.5 (m, 4H, aromatic ring, NH). ESI-MS: 207 (MH^+).

***N*-Methyl-*N*-(2,3,3-trimethyl-3*H*-indol-5-yl)acetamide (16) and *N*-Methyl-*N*-(2-methyl-1,3-benzothiazol-6-yl)acetamide (17).** The acetamide (**14** or **15**) from the previous synthesis (2.00 mmol) was dissolved in 30 mL of methyl sulfoxide. Sodium hydride (60% suspension in mineral oil, 2.20 mmol) was added to this solution in small portions with stirring. Hydrogen was evolved, and the mixture was kept at room temperature for 30 min. Then, methyl iodide (2.2 mmol) in dimethyl sulfoxide was added dropwise over 10 min. When addition was complete, the mixture was stirred at room temperature for 1 h, then diluted with water (100 mL). Organics were extracted with methylene chloride (3 × 50 mL). The combined organic layers were washed with water (2 × 50 mL) and dried. Evaporation of solvent gave *N*-methylacetamides, which were purified by chromatography on silica using ethyl acetate as eluent.

***N*-Methyl-*N*-(2-methyl-1,3-benzothiazol-6-yl)acetamide (16).** The yield was 87%, white solid. ^{1}H NMR (500 MHz, DMSO-d_6): δ 1.87 (s, 3H, $COCH_3$), 2.84 (s, 3H, CH_3), 3.29 (s, 3H, NCH_3), 7.3−8.5 (m, 3H, aromatic ring). ESI-MS: 221 (MH^+).

***N*-Methyl-*N*-(2,3,3-trimethyl-3*H*-indol-5-yl)acetamide (17).** The yield was 72%, white solid. ^{1}H NMR (500 MHz, $CDCl_3$): δ 1.31 (s, 6H, 2×CH_3), 1.85 (s, 3H, $COCH_3$), 2.29 (s, 3H, CH_3), 3.26 (s, 3H, NCH_3), 7.1−7.6 (m, 3H, aromatic ring). ESI-MS: 231 (MH^+).

***N*,2-Dimethyl-1,3-benzothiazol-6-amine (18) and *N*,2,3,3-Tetramethyl-3*H*-indol-5-amine (19).** Methylacetamide (**18** or **19**) from the previous synthesis (1.5 mmol) was mixed with concentrated hydrochloric acid (10 mL), and the mixture was stirred under reflux for 4 h. After cooling, a solution of 6 g of sodium hydroxide in 50 mL of water was added to the mixture. The separated organics were extracted with methylene chloride (3 × 50 mL). The combined organic extracts were washed with water (2 × 50 mL) and dried. Evaporation of solvent gave crude methylamines, which were purified by column chromatography on silica using ethyl acetate as eluent.

***N*,2-Dimethyl-1,3-benzothiazol-6-amine (18).** The yield was 90%, white solid. ^{1}H NMR (500 MHz, $CDCl_3$): δ 2.82 (s, 3H, CH_3), 2.94 (s, 3H, NCH_3), 3.7 (bs, 1H, NH), 6.8−7.3 (m, 3H, aromatic ring). ESI-MS: 179 (MH^+).

***N*,2,3,3-Tetramethyl-3*H*-indol-5-amine (19).** The yield was 86%, yellow solid. ^{1}H NMR (500 MHz, $CDCl_3$): δ 1.34 (s, 6H, 2×CH_3), 2.29 (s, 3H, CH_3), 2.94 (s, 3H, NCH_3), 3.52 (s, 1H, NH), 6.5−7.5 (m, 3H, aromatic ring). ESI-MS: 189 (MH^+).

{2-[Methyl(2,3,3-trimethyl-3*H*-indol-5-yl)amino]-2-oxoethoxy}-acetic Acid (20) and {2-[Methyl(2-methyl-1,3-benzothiazol-6-yl)-amino]-2-oxoethoxy}acetic Acid (21). *N*-Methylamine from the previous synthesis (1.0 mmol) was dissolved in 20 mL of chloroform. A 1.1 mmol sample of diglycolic anhydride was added, and the mixture was stirred under reflux for 2 h. After cooling, the solvent was evaporated. The solid was recrystallized from acetone to give pure acids.

{2-[Methyl(2,3,3-trimethyl-3*H*-indol-5-yl)amino]-2-oxoethoxy}-acetic Acid (20). The yield was 75%, white powder. ^{1}H NMR (500 MHz, $CDCl_3$): δ 1.33 (s, 6H, 2×CH_3), 2.32 (s, 3H, CH_3), 3.33 (s, 3H, NCH_3), 4.05 (s, 2H, CH_2CON), 4.15 (s, 2H, CH_2COOH), 3.52 (s, 1H, NH), 7.1−7.7 (m, 3H, aromatic ring). ESI-MS: 305 (MH^+).

{2-[Methyl(2-methyl-1,3-benzothiazol-6-yl)amino]-2-oxoethoxy}-acetic Acid (21). The yield was 82%, white powder. ^{1}H NMR (500 MHz, DMSO-d_6): δ 2.80 (s, 3H, CH_3), 3.21 (s, 3H, NCH_3), 3.94 (s, 2H, CH_2CON), 4.03(s, 2H, CH_2COOH), 7.4−8.2 (m, 3H, aromatic ring). ESI-MS: 295 (MH^+).

3-{5-[[(Carboxymethoxy)acetyl](methyl)amino]-2,3,3-trimethyl-3*H*-indolium-1-yl}propane-1-sulfonate (22) and 3-{6-[[(Carboxymethoxy)acetyl](methyl)amino]-2-methyl-1,3-benzothiazol-3-ium-3-yl}propane-1-sulfonate (23). To a solution of acid (**21** or **22**, 1.00 mmol) in 25 mL of dry acetonitrile was added propane sulfone (10 mmol). This mixture was stirred under reflux for 48 h. After cooling the hygroscopic salt was filtered, washed with acetone, and immediately used in the next step.

3-{5-[[(Carboxymethoxy)acetyl](methyl)amino]-2,3,3-trimethyl-3*H*-indolium-1-yl}propane-1-sulfonate (22). The yield was 72%, white solid. ESI-MS: 427 (MH^+).

3-{6-[[(Carboxymethoxy)acetyl](methyl)amino]-2-methyl-1,3-benzothiazol-3-ium-3-yl}propane-1-sulfonate (23). The yield was 64%, white solid. ESI-MS: 417 (MH^+).

Sodium 3-{(2*Z*)-5-{[(Carboxymethoxy)acetyl]methylamino}-2-[(2*E*,4*Z*)-4-(1,1-dioxido-3-oxo-1-benzothien-2(3*H*)-ylidene)but-2-enylidene]-3,3-dimethyl-2,3-dihydro-1*H*-indol-1-yl}propane-1-sulfonate (24) and Sodium 3-{(2*Z*)-6-{[(Carboxymethoxy)acetyl]-methylamino}-2-[(2*E*,4*Z*)-4-(1,1-dioxido-3-oxo-1-benzothien-2(3*H*)-ylidene)but-2-enylidene]-1,3-benzothiazol-3(2*H*)-yl} propane-1-sulfonate (25). A mixture of the quaternary salt (**22** or **23**, 0.5 mmol) and enol ether **9** (0.625 g, 2.50 mmol) in 20 mL of a chloroform−acetic acid mixture (1:1) was magnetically stirred at 60 °C under nitrogen. A solution of 0.200 g of sodium acetate in 5 mL of acetic acid was added by drops to the reaction mixture. The stirring was continued for an additional 24 h. After cooling the dye **25** crystallized from the reaction mixture and was separated by filtration and purified by recrystallization from acetic acid. The reaction mixture containing dye **24** was evaporated in a vacuum, and the pure dye was isolated by chromatography over silica gel, eluting with acetone−acetic acid (5:1), followed by recrystallization from acetic acid.

Sodium 3-{(2*Z*)-5-{[(Carboxymethoxy)acetyl]methylamino}-2-[(2*E*,4*Z*)-4-(1,1-dioxido-3-oxo-1-benzothien-2(3*H*)-ylidene)but-2-enylidene]-3,3-dimethyl-2,3-dihydro-1*H*-indol-1-yl}propane-1-sulfonate (24). The yield was 60%. ^{1}H NMR (500 MHz, DMSO-d_6): δ 1.69 (s, 6H, 2×CH_3), 2.04 (p, $^3J_{H-H}$ = 7.0 Hz, 2H, $CH_2-CH_2-CH_2$), 2.65 (t, $^3J_{H-H}$ = 7.0 Hz, 2H, CH_2-SO_3), 3.25 (s, 3H, CH_3N), 4.05 (bs, 2H, CH_2COOH), 4.19 (bs, 2H, CH_2CON), 4.24 (t, $^3J_{H-H}$ = 7.0 Hz, 2H, CH_2-N), 6.4−8.5 (m, 11H). MALDI-FTMS: MNa^+ found 689.1203, expected 689.1210.

Sodium 3-{(2*Z*)-6-{[(Carboxymethoxy)acetyl]methylamino}-2-[(2*E*,4*Z*)-4-(1,1-dioxido-3-oxo-1-benzothien-2(3*H*)-ylidene)but-2-enylidene]-1,3-benzothiazol-3(2*H*)-yl} propane-1-sulfonate (25). The yield was 54%. ^{1}H NMR (500 MHz, DMSO-d_6): δ 2.09 (p, $^3J_{H-H}$ = 7.0 Hz, 2H, $CH_2-CH_2-CH_2$), 2.67 (t, $^3J_{H-H}$ = 7.0 Hz, 2H, CH_2-SO_3), 3.27 (s, 3H, CH_3), 4.09 (bs, 2H, CH_2COOH), 4.17 (bs, 2H, CH_2CON), 4.57 (t, $^3J_{H-H}$ = 7.0 Hz, 2H, CH_2-N), 6.8−8.0 (m, 11H). ESI-MS: 635 $(M - Na + 2H)^+$.

Sodium 3-{(2*Z*)-5-[({2-[(2,5-Dioxopyrrolidin-1-yl)oxy]-2-oxoethoxy}acetyl)methylamino]-2-[(2*E*,4*Z*)-4-(1,1-dioxido-3-oxo-1-benzothien-2(3*H*)-ylidene)but-2-enylidene]-3,3-dimethyl-2,3-dihydro-1*H*-indol-1-yl}propane-1-sulfonate (I-SO-OSu, 4f) and Sodium 3-[(2*E*)-6-[({2-[(2,5-Dioxopyrrolidin-1-yl)oxy]-2-oxoethoxy}acetyl)-methylamino]-2-[(2*E*,4*Z*)-4-(1,1-dioxido-3-oxo-1-benzothien-2(3*H*)-ylidene)but-2-enylidene]-1,3-benzothiazol-3(2*H*)-yl]propane-1-sulfonate (S-SO-OSu, 2f). To a solution of 0.50 mmol of free acid dye from the previous synthesis in 10 mL of dimethylformamide were added tetramethyl(succinimido)uronium tetrafluoroborate (301 mg, 1.00 mmol) and diisopropylethylamine (200 mg). The solution was stirred under nitrogen at room temperature for 1 h. The solvent was removed under high vacuum. The residue was treated with acetone (5 mL), and ether (25 mL) was added to precipitate the reactive dye.

Sodium 3-{(2*Z*)-5-[({2-[(2,5-Dioxopyrrolidin-1-yl)oxy]-2-oxoethoxy}acetyl)methylamino]-2-[(2*E*,4*Z*)-4-(1,1-dioxido-3-oxo-1-benzothien-2(3*H*)-ylidene)but-2-enylidene]-3,3-dimethyl-2,3-dihydro-1*H*-indol-1-yl}propane-1-sulfonate (I-SO-OSu, 4f). The yield was 90%. ^{1}H NMR (500 MHz, DMSO-d_6): δ 1.69 (s, 6H, 2×CH_3), 2.04 (p, $^3J_{H-H}$ = 7.0 Hz, 2H, $CH_2-CH_2-CH_2$), 2.65 (t, $^3J_{H-H}$ = 7.0 Hz, 2H, CH_2-SO_3), 2.92 (s, 4H, CH_2CH_2), 3.25 (s, 3H, CH_3N), 4.12−4.17 (m, 4H, CH_2CON, CH_2COOSu), 4.24 (t, $^3J_{H-H}$ = 7.0 Hz, 2H, CH_2-N), 6.4−8.5 (m, 11H). ESI-MS: 742 $(M - Na + 2H)^+$.

Sodium 3-[(2*E*)-6-[({2-[(2,5-Dioxopyrrolidin-1-yl)oxy]-2-oxoethoxy}-acetyl)methylamino]-2-[(2*E*,4*Z*)-4-(1,1-dioxido-3-oxo-1-benzothien-2(3*H*)-ylidene)but-2-enylidene]-1,3-benzothiazol-3(2*H*)-yl]propane-1-sulfonate (S-SO-OSu, 2f). The yield was 87%. ^{1}H NMR (500 MHz, DMSO-d_6): δ 2.09 (p, $^3J_{H-H}$ = 7.0 Hz, 2H, $CH_2-CH_2-CH_2$), 2.67 (t, $^3J_{H-H}$ = 7.0 Hz, 2H, CH_2-SO_3), 2.80 (s, 4H, CH_2CH_2), 3.26 (s, 3H, CH_3), 4.13−4.19 (m, 4H, CH_2CON CH_2COOSu), 4.57 (t, $^3J_{H-H}$ = 7.0 Hz, 2H, CH_2-N), 6.4−8.4 (m, 11H). ESI-MS: 732 $(M - Na + 2H)^+$.

Preparation of Sodium 3-[(2*Z*)-6-(Acetylamino)-2-[(2*E*)-4-(1,3-dimethyl-4,6-dioxo-2-thioxotetrahydropyrimidin-5(2*H*)-ylidene)but-2-enylidene]-1,3-benzothiazol-3(2*H*)-yl]propane-1-sulfonate (1g). The suspension of dye **1e** (200 mg) in 10 mL of acetic anhydride was stirred at 80 °C for 12 h under nitrogen. After cooling the crude dye was separated by filtration and purified by recrystallization from methanol. The yield was 120 mg (55%). ^{1}H NMR (400 MHz, DMSO-d_6): δ 1.90 (s, 3H, CH_3CO), 2.00 (p, $^3J_{H-H}$ = 7.0 Hz, 2H, $CH_2-CH_2-CH_2$), 2.55 (t, $^3J_{H-H}$ = 7.0 Hz, 2H, CH_2-SO_3), 3.61 (s, 6H, 2×CH_3), 4.56 (t, $^3J_{H-H}$ = 7.0 Hz, 2H, CH_2-N), 6.8−7.8 (m, 7H), 10.56 (1H, NH). MALDI-FTMS: MH^+ found 559.0762, expected 559.075.

Preparation of Dyes 1h, 2g, and 4g. Reactions of Iodoacetamides 1f, 2e, and 4e with 2-Mercaptoethanol. A 30 mg sample of iodoacetamido dye (**1f**, **2e**, **4e**) was added to a solution of 2-mercaptoethanol (30 mg) in 2.0 mL of $NaHCO_3-Na_2CO_3$ buffer (pH = 8.0), and the mixture was stirred for 2 h at room temperature. Silica gel TLC (MeOH−H_2O, 90:10) showed complete consumption of starting dye. The conjugates were isolated by chromatography on a C18 column using a water−acetonitrile gradient.

Sodium 3-[(2*Z*)-6-({[(2-Hydroxyethyl)thio]acetyl}amino)-2-[(2*E*)-4-(1,3-dimethyl-4,6-dioxo-2-thioxotetrahydropyrimidin-5(2*H*)-ylidene)-but-2-enylidene]-1,3-benzothiazol-3(2*H*)-yl]propane-1-sulfonate (1h). ^{1}H NMR (500 MHz, DMSO-d_6): δ 2.03 (p, $^3J_{H-H}$ = 7.0 Hz, 2H, $CH_2-CH_2-CH_2$), 2.65 (t, $^3J_{H-H}$ = 7.0 Hz, 2H, CH_2-SO_3), 2.80 (t, $^3J_{H-H}$ = 6.6 Hz, 2H, CH_2S), 3.40 (s, 2H, $COCH_2S$), 3.60 (s, 6H, 2×CH_3), 3.64 (q, $^3J_{H-H}$ = 6.6 Hz, 2H, CH_2-OH), 4.57 (t, $^3J_{H-H}$ = 7.0 Hz, 2H, CH_2-N), 4.94 (bs, 1H, OH), 6.8−8.0 (m, 11H), 10.47 (s, 1H, NHCO). ESI-MS: 613 $(M - Na + 2H)^+$.

Sodium 3-[(2*Z*)-6-({[(2-Hydroxyethyl)thio]acetyl}amino)-2-[(2*E*,4*Z*)-4-(1,1-dioxido-3-oxo-1-benzothien-2(3*H*)-ylidene)but-2-enylidene]-1,3-benzothiazol-3(2*H*)-yl]propane-1-sulfonate (2g). ^{1}H NMR (500 MHz, DMSO-d_6): δ 2.08 (p, $^3J_{H-H}$ = 7.0 Hz, 2H, $CH_2-CH_2-CH_2$), 2.66 (t, $^3J_{H-H}$ = 7.0 Hz, 2H, CH_2-SO_3), 2.79 (t, $^3J_{H-H}$ = 6.6 Hz, 2H, SCH_2-CH_2), 3.47 (s, 2H, $COCH_2S$), 3.64 (q, $^3J_{H-H}$ = 6.6 Hz, 2H, CH_2OH), 4.57 (t, $^3J_{H-H}$ = 7.0 Hz, 2H, CH_2-N), 4.95 (t, $^3J_{H-H}$ = 6.6 Hz, 1H, OH), 6.6−8.5 (m, 11H), 10.50 (s, 1H, NHCO). MALDI-FTMS: MH^+ found 645.0464, calculated 645.0458.

Sodium 3-{(2*E*)-5-({[(2-Hydroxyethyl)thio]acetyl}amino)-2-[(2*E*,4*Z*)-4-(1,1-dioxido-3-oxo-1-benzothien-2(3*H*)-ylidene)but-2-enylidene]-3,3-dimethyl-2,3-dihydro-1*H*-indol-1-yl}propane-1-sulfonate (4g). ^{1}H NMR (500 MHz, DMSO-d_6): δ 1.70 (s, 6H, 2×CH_3), 2.08 (p, $^3J_{H-H}$ = 6.9 Hz, 2H, $CH_2-CH_2-CH_2$), 2.67 (t, $^3J_{H-H}$ = 6.9 Hz, 2H, CH_2-SO_3), 2.81 (t, $^3J_{H-H}$ = 6.6 Hz, 2H, CH_2-CH_2S), 3.43 (s, 2H, $COCH_2S$), 4.26 (t, $^3J_{H-H}$ = 6.9 Hz, 2H, CH_2-N), 6.4−8.3 (m, 11H), 10.31 (s, 1H, NHCO). MALDI-FTMS: MNa^+ found 677.1032, calculated 677.1028.

Protein Labeling. A fragment of Wiskott Aldrich Syndrome Protein (WASP, residues 201−320), mutated to contain a single cysteine (F271C), was labeled with S-SO-IAA, Cy3,[71] or Cy5[71] dyes. A stock solution of the dye in DMSO (10−20 mM) was added to 200 μL of protein solution (200 μM in sodium phosphate buffer, pH = 7.5) to produce a final dye concentration of 1−2 mM. The reaction mixture was incubated for 4 h at room temperature, then quenched by addition of 1 μL of mercaptoethanol. The reaction mixture was spun at 12 000 rpm for 2 min to remove any precipitates that might have formed during the reaction, and the supernatant was purified using G25 sepharose gel filtration. The dye−protein adduct was clearly separated from free dye during gel filtration. Purity of the conjugates was confirmed by SDS-PAGE electrophoresis. No free dye was seen in purified protein conjugates. Control samples of free dye were clearly visible on the gel at lower MW than protein. Conjugates formed single, highly colored

(71) Toutchkine, A.; Nalbant, P.; Hahn, K. M. *Bioconj. Chem.* **2002**, *13*, 387−391.

fluorescent protein bands with molecular weights corresponding to the WASP fragment. The dye-to-protein ratio was calculated by measuring protein and dye concentrations using absorbance spectroscopy as previously described.[25,72] In each case this ratio was between 0.9 and 1.0. Concentration of CBD was independently confirmed by Coomassie Plus assay (Pierce) calibrated with bovine serum albumin as a standard. Aliquots of the labeled CBD (15−50 μM) were stored at −80 °C. No significant loss of binding ability was observed after 6 months of storage.

Analysis of Cdc42 Activation. A solution of the WASP conjugate (300 nM) in a assay buffer (50 mM TrisHCl, pH 7.6, 50 mM NaCl, 5 mM $MgCl_2$, 1 mM DTT) was mixed 1:1 (v/v) with solutions of Cdc42, preequilibrated with 10 mM GDP or GTPγS as described.[73] Emission at 630 nm and excitation at 600 nm were used to acquire excitation and emission spectra, respectively. For nucleotide dependence, Cdc42 (500 nM) was preincubated with varying concentrations of GTPγS (1−500 nM).

(72) Haugland, R. P. *Handbook of Fluorescent Probes and Research Chemicals*; Molecular Probes Inc.: Eugene, OR, 1996.
(73) Knaus, U. G.; Heyworth, P. G.; Kinsella, B. T.; Curnutte, J. T.; Bokoch, G. M. *J. Biol. Chem.* **1992**, *267*, 23575−23582.

Photobleaching. All samples contained 1 mM dye in a final volume of 10 mL. For nitrogen and oxygen saturation the samples were bubbled with solvent-saturated gas for 30 min. A 90 W halogen tungsten lamp was employed for irradiation, with a fan used for cooling. The temperature of samples was 25 ± 1 °C during reactions. The absorption spectrum of each sample was measured before irradiation and after every 10 h period. For the trapping experiment thioanisole (1.0 M) was added to oxygen-saturated butanol solution of dye **1b**. After 60 h of irradiation the reaction mixture was analyzed by GC−MS for products formed. The products, methylphenylsulfoxide and methylphenyl sulfone, were identified by comparison with authentic samples.

Acknowledgment. We are grateful to Dr. Perihan Nalbant for help with preparation of Cy3 and Cy5−WASP fragment conjugates. We thank the NIH (R01-AG-15430 and R01-GM-57464), Novartis AG, the Leukemia and Lymphoma Society (Grant 3427-02 to A.T.), and the Arthritis Foundation (V.K.) for supporting this work.

JA0290882